

# Insulin-induced vascular redox dysregulation in human atherosclerosis is ameliorated by dipeptidyl peptidase 4 inhibition

Ioannis Akoumianakis<sup>1</sup>, Ileana Badi<sup>1</sup>, Gillian Douglas<sup>1</sup>, Surawee Chuaiphichai<sup>1</sup>, Laura Herdman<sup>1</sup>, Nadia Akawi<sup>1</sup>, Marios Margaritis<sup>1</sup>, Alexios S. Antonopoulos<sup>1</sup>, Evangelos K. Oikonomou<sup>1</sup>, Costas Psarros<sup>1</sup>, Nikolaos Galiatsatos<sup>2</sup>, Dimitris Tousoulis<sup>3</sup>, Attila Kardos<sup>4</sup>, Rana Sayeed<sup>5</sup>, George Krasopoulos<sup>5</sup>, Mario Petrou<sup>5</sup>, Uwe Schwahn<sup>6</sup>, Paulus Wohlfart<sup>6</sup>, Norbert Tennagels<sup>6</sup>, Keith M. Channon<sup>1</sup>, Charalambos Antoniades<sup>1\*</sup>

## Affiliations:

<sup>1</sup> Division of Cardiovascular Medicine, Radcliffe Department of Medicine, University of Oxford, UK, OX3 9DU

<sup>2</sup> Biochemistry Department, Hippokration General Hospital, Athens, Greece , 115 27

<sup>3</sup> First Cardiology Clinic, Athens University Medical School, Greece , 115 27

<sup>4</sup> Milton Keynes University Hospital NHS Foundation Trust & Faculty of Life Sciences University of Buckingham, UK, MK6 5LD

<sup>5</sup> Cardiothoracic Surgery Department, Oxford University Hospitals NHS Foundation Trust, UK, OX3 9DU

<sup>6</sup> Sanofi Aventis Deutschland GmbH, Germany, D-65926

**\*Corresponding author.** E-mail: antoniad@well.ox.ac.uk

**Single-sentence summary:** Insulin causes vascular oxidative stress in human atherosclerosis that is reversed by restoring vascular insulin sensitivity using a dipeptidyl-peptidase-4 inhibitor.

\*This manuscript has been accepted for publication in Science Translational Medicine. This version has not undergone final editing. Please refer to the complete version of record at [www.sciencetranslationalmedicine.org/](http://www.sciencetranslationalmedicine.org/). The manuscript may not be reproduced or used in any manner that does not fall within the fair use provisions of the Copyright Act without the prior written permission of AAAS.

## Abstract

Recent clinical trials have revealed that aggressive insulin treatment has a neutral effect on cardiovascular risk in patients with diabetes despite improved glycemic control, which may suggest confounding direct effects of insulin on the human vasculature. We studied 580 patients with coronary atherosclerosis undergoing coronary bypass surgery (CABG), discovering that high endogenous insulin was associated with reduced nitric oxide (NO) bioavailability *ex vivo* in vessels obtained during surgery. *Ex vivo* experiments with human internal mammary arteries and saphenous veins obtained from 94 patients undergoing CABG revealed that both long-acting insulin analogues and human insulin triggered abnormal responses of post-insulin receptor substrate 1 (IRS1) downstream signalling *ex vivo*, independently of systemic insulin resistance status. These abnormal responses led to reduced NO bioavailability, activation of NADPH-oxidases, and uncoupling of endothelial NO synthase. Treatment with an oral dipeptidyl peptidase 4 inhibitor (DPP4i) *in vivo* or DPP4i administered to vessels *ex vivo* restored physiological insulin signalling, reversed vascular insulin responses, reduced vascular oxidative stress, and improved endothelial function in humans. The detrimental effects of insulin on vascular redox state and endothelial function and insulin-sensitizing effect of DPP4i were also validated in high fat diet-fed ApoE<sup>-/-</sup> mice treated with DPP4i. High plasma DPP4 activity and high insulin were additively related with higher cardiac mortality in patients with coronary atherosclerosis undergoing CABG. These findings may explain the inability of aggressive insulin treatment to improve cardiovascular outcomes, raising the question whether vascular insulin sensitization with DPP4i should precede initiation of insulin treatment and continue as part of a long-term combination therapy.

## Introduction:

Type 2 diabetes mellitus is a global health epidemic and an important driver of cardiovascular complications (1). This is believed to result from hyperglycaemia, which has crucial and profound effects on the human vasculature (2). Such effects range from vascular protein kinase C activation, glycation of a variety of important proteins such as Akt (3), advanced glycation end-product (AGE) formation, and downstream AGE signalling and dysregulation of vascular redox signalling by affecting the activity of enzymes such as NADPH-oxidases and the coupling status of endothelial nitric oxide synthase (eNOS) (2, 4). Despite the important vascular effects of hyperglycaemia and the protective effect of standard glycemic control on cardiovascular clinical endpoints, aggressive glucose lowering with insulin analogues has failed to further improve cardiovascular outcomes in type 2 diabetes, despite achieving optimal glycemic control (5-7), suggesting that the cardiovascular benefit of glucose lowering in diabetes is limited to changes at the high end of the serum glucose range. The ACCORD clinical trial was the first landmark study to display no cardiovascular risk (mortality, and non-fatal events such as myocardial infarction) benefit after intensive glycemic control largely by insulin-based treatments (8), suggesting glycemic control is not sufficient to prevent vascular complications, and local vascular parameters should be considered.

The vascular effects of insulin involve downstream activation of insulin receptor substrate 1 (IRS1) (9), leading to potential activation of the PI3K/Akt pathway or the MAPK pathway (9). Akt signalling has been associated with the ability of insulin to activate eNOS and increase NO bioavailability (10). However, it is unclear how insulin vascular signalling changes in diabetes and human atherosclerosis, because mechanistic data available are focused on either in vitro cell culture or in vivo animal models.

The dipeptidyl peptidase 4 (DPP4) protease cleaves proline dipeptides from the N-terminus of polypeptides including glucagon-like peptide 1 (GLP1), a peptide with glucose-lowering abilities (11). It is now evident that DPP4 inhibitors ameliorate cellular insulin resistance (IR) in experimental models (11), but their effects on insulin signalling in the human vascular wall is unknown.

In this study, we explored the direct effects of human and synthetic insulins on redox signalling and NO bioavailability in human arteries and veins from patients with coronary atherosclerosis. We hypothesized that vascular IR may be responsible for the inability of aggressive insulin treatment to reduce cardiovascular risk in patients with diabetes. We investigated the potential role of insulin sensitization strategies in restoring physiological insulin signalling in the human vascular wall.

## **Results**

### **Effects of insulin on vascular redox state in patients with atherosclerosis**

We first investigated the association between circulating insulin and endothelial function in non-diabetic patients undergoing coronary artery bypass surgery (CABG) (Study 1, Table 1 and table S1). High serum insulin was associated with reduced vasorelaxations of human vessels (saphenous veins, SV) in response to acetylcholine (ACh, Fig. 1A) and bradykinin (Bk, Fig. 1B), but not to sodium nitroprusside (SNP, Fig. 1C), suggesting an inverse association between serum insulin and NO bioavailability in the human endothelium. To explore whether the inverse association between insulin and endothelial function is causal, we then exposed human vessels from atherosclerosis patients with diabetes and without diabetes or evidence of systemic IR (HOMA-IR<2.9) to exogenous insulin *ex vivo*, using both long-acting insulin analogues (M1 metabolite of glargine or degludec), and human insulin (Study 2, Table 1). All

insulin types significantly reduced vasorelaxations in response to ACh but not to SNP in all patient vessels (Fig. 1, D to G for insulin glargine; fig. S1 for insulin degludec and human insulin), suggesting a class effect of insulin on the vascular wall, even in the absence of diabetes or systemic IR.

To understand how insulin could cause endothelial dysfunction in vessels from patients with vascular disease, we then explored the interactions between insulin and vascular redox state in patients without diabetes from Study 1 (to avoid treatment confounding in diabetic patients). We observed that increased serum insulin was associated with increased NADPH-oxidases activity in human vessels [internal mammary arteries (IMA) and SV], evidenced by increased NADPH-stimulated  $O_2^-$  and particularly Vas2870-inhibitable  $O_2^-$  production from these vessels as measured by lucigenin chemiluminescence (fig. S2). Vas2870 is a pan-NOX inhibitor of NADPH-oxidases. To examine whether exogenous insulin administration could causally increase oxidative stress in the human vascular wall, we first exposed human IMA and SV (obtained from patients in Study 2) to human insulin, insulin glargine M1, and insulin degludec in a screening dose-response experiment. We observed that all insulin types increased vascular basal, NADPH-stimulated, and Vas2870-inhibitable  $O_2^-$  (fig. S3). Human insulin and M1 glargine had that effect at concentrations  $\geq 10$  nM whereas degludec displayed similar effect at 100 nM (fig. S3). This is in agreement with the described pharmacodynamic properties of these insulin types, considering that M1 glargine is very similar to human insulin and degludec is less potent than the other two (12-14).

Further incubations with insulin glargine M1, used as a representative insulin analogue and named as “insulin” in the subsequent results sections, *ex vivo* demonstrated that insulin (10 nM) increased  $O_2^-$  generation in both SV and IMA from patients with diabetes as well as and from patients without diabetes or systemic IR, which is comparable to the *in vivo* situation (serum insulin median[25th-75th percentile]: 5.5[3.4-8.3] nM in Study 1; Fig. 2, A to C for SV

and D to F for IMA; fig. S4, A to C for human insulin). This was due to activation of vascular NADPH oxidases as documented by the increase of NADPH-stimulated as well as the Vas2870-inhibitable  $O_2^-$  production. These findings were replicated using DHE staining on intact IMA segments treated with insulin in the presence or absence of Vas2870 (Fig. 2G). Complementary to this, long-term insulin treatment for 8h activated several pro-inflammatory pathways in human IMA, further supporting a potentially detrimental direct effect of insulin on the vascular wall of patients with atherosclerosis (fig. S5).

To test whether these observations on the effects of insulin on human vessels were associated with the presence of vascular disease, we exposed mouse aortas from healthy wild-type animals to the same protocol of insulin treatment *ex vivo*. We observed that insulin reduced vascular  $O_2^-$  in the mouse aortas by reducing NADPH-oxidases activity by 50-70%, providing a positive control for the study intervention (Fig. 2, H to J; fig. S6, A to C).

### **DPP4 inhibition restores vascular redox responses to insulin in human atherosclerosis**

Our results so far suggest that insulin has a class stimulatory effect on vascular NADPH-oxidases in human atherosclerosis, independently of the presence of diabetes or systemic IR. To explore whether an insulin sensitizing intervention like DPP4 inhibitor (DPP4i) treatment would reverse these effects, we selected patients receiving chronic treatment with oral DPP4i and exposed their IMA to insulin *ex vivo*. We observed a striking reversal of the effects of insulin on vascular redox state, suppressing NADPH oxidase activity and vascular  $O_2^-$  generation (Fig. 3, A to C). This was not observed with metformin, a common antidiabetic medication with insulin-sensitizing properties (15) (fig. S7), suggesting that DPP4i may have strong vasculature-specific effects. To examine whether DPP4i acts directly on the human arterial wall to reverse the effects of insulin on vascular redox state, we exposed human arteries

and veins to insulin *ex vivo* in the presence or absence of KR62436, a synthetic DPP4i. We found that insulin alone stimulated  $O_2^{\cdot -}$  production in both human IMA and SVs, whereas pre-incubation of rings from the same vessels with KR62436 reversed their vascular responses to insulin, leading to reduced vascular  $O_2^{\cdot -}$  in response to exogenous insulin administration by suppressing the activity of NADPH-oxidases (Fig. 3, D to I; fig. S8, A to F). DPP4i had no direct antioxidant or  $O_2^{\cdot -}$ -scavenging properties, as evidenced by its neutral effect on xanthine oxidase (XO)-derived  $O_2^{\cdot -}$ , which is used as a chemical protocol to evaluate direct  $O_2^{\cdot -}$ -scavenging properties (fig. S9). These findings suggest that DPP4 inhibition in the human vascular wall restores physiological responses of vascular redox signaling to exogenous insulin administration. Crucially, insulin administered to ApoE<sup>-/-</sup> mice [fed with high fat diet (HFD) for 4 weeks to stimulate cardiometabolic disease], increased basal, NADPH-stimulated, and Vas2870-inhibitable  $O_2^{\cdot -}$  measured in aortic tissue, all of which were reversed by 4-week pre-treatment with linagliptin (a clinically used DPP4i) during the course of HFD (fig. S10, A to C). This provides an *in vivo* validation of the proof-of-concept that cardiometabolic disease is characterized by vascular IR which can be rescued by oral DPP4i treatment.

To understand the underlying mechanisms by which insulin and DPP4 regulate NADPH-oxidases activity in human vessels, we explored their direct effects on the regulatory subunit of NOX1 and NOX2 isoforms of NADPH oxidases, Rac1. Insulin activated Rac1 (Fig. 3J), triggering its membrane translocation together with the p47<sup>phox</sup> subunit of the enzymes (Fig. 3, K and L). These effects were reversed after pre-treatment of these vessels with DPP4i, in which case insulin led to GTP-Rac1 induction and prevented the membrane translocation of Rac1 and p47<sup>phox</sup> (Fig. 3, J to L). DPP4 inhibition had no direct effects on Rac1 activation or Rac1/p47<sup>phox</sup> membrane translocation (Fig. 3, J to L). In agreement with these findings, high circulating DPP4 activity was positively associated with vascular  $O_2^{\cdot -}$  generation (basal, NADPH-stimulated, and Vas2870-inhibitable) in human vessels (fig. S11). These findings

imply that targeting DPP4 in patients with diabetes may restore physiological vascular insulin signaling, at least in the presence of advanced atherosclerosis.

### **DPP4 inhibition modulates the effects of exogenous insulin on eNOS in human vessels**

To better understand how exogenous insulin controls vascular redox state in human vessels, we next investigated the direct effects of insulin on vascular NO bioavailability and eNOS coupling in vessels from patients with atherosclerosis. Insulin directly induced vascular eNOS uncoupling, documented by a striking increase in LNAME-inhibitable  $O_2^{\cdot-}$  (Fig. 4A). This suggests that insulin turns eNOS from a source of NO to a source of  $O_2^{\cdot-}$ , further dysregulating vascular redox signaling. Treatment of these vessels with DPP4i reversed the effects of insulin on eNOS coupling (Fig. 4A), confirming that insulin treatment together with DPP4i improves vascular redox signaling by restoring eNOS coupling in human atherosclerosis.

Given that insulin has been shown to affect eNOS activity via Akt-mediated ser1177 phosphorylation in vitro (10), we next explored the effects of insulin on eNOS phosphorylation status in humans with vascular disease. We found that insulin alone did not induce eNOS phosphorylation at the activation site Ser1177, whereas significant Ser1177 phosphorylation was induced by insulin in the presence of DPP4i (Fig. 4B). In contrast, insulin increased eNOS phosphorylation at ser1177 in human umbilical vein endothelial cells used as a biological positive control, whereas DPP4i conveyed no additional benefit in these cells (Fig. 4C). These findings highlight the discrepancy in vascular insulin responses between humans with vascular disease and disease-free in vitro and in vivo models.

To understand how insulin induces eNOS uncoupling, we quantified vascular eNOS co-factor tetrahydrobiopterin (BH4), a key regulator of eNOS coupling. Indeed, insulin reduced BH4 bioavailability without affecting total biopterins content [that includes dihydrobiopterin (BH2)

and biopterin (B)], resulting in reduced BH4/total biopterins ratio (Fig. 4, D to F). This finding suggests that insulin induces BH4 oxidation without affecting its biosynthesis, leading to eNOS uncoupling by changing the stoichiometry between BH4 and BH2/B (Fig. 4, D to F). Conversely, in the presence of DPP4i, insulin increased vascular BH4 content and the ratio of BH4/total biopterins, improving eNOS coupling (Fig. 4, D to F).

Given that, in the presence of DPP4i, insulin can improve eNOS coupling and activate eNOS, we then hypothesized that it would also improve endothelial function in human vessels. Indeed, we found that insulin impaired the vasorelaxations of human vessels to ACh, whereas insulin had the opposite effect in the presence of a DPP4i, improving ACh-induced vasorelaxations (Fig. 4G). These effects were endothelium-specific and did not affect the endothelium-independent vasorelaxations to SNP (Fig. 4H). DPP4i alone did not affect the relaxations of these vessels to ACh or SNP, confirming its role as a modulator of insulin signaling in human vessels. Insulin also impaired endothelium-dependent ACh vasorelaxations in the aortas of HFD-fed ApoE<sup>-/-</sup> mice, an effect abolished by oral linagliptin, whereas there were no differences in endothelium-independent vasorelaxations between the aortas of treated vs control mice in the absence of insulin stimulation (fig. S12).

### **Characterizing abnormal vascular insulin signaling in humans with vascular disease**

Given that insulin induces oxidative stress and endothelial dysfunction in vessels from patients with atherosclerosis, we hypothesized that these dysregulated vascular redox responses to insulin could reflect abnormal downstream insulin signaling, representing a default state of vascular IR in these human vessels, even in patients with no evidence of IR or diabetes. To understand the nature of these unexpected responses, we investigated the balance between phosphorylation (activation) of vascular Akt vs Erk1&2, as representative downstream

mediators of the two insulin signaling axes dysregulated in IR. We observed that in vessels from our patients, insulin failed to stimulate Akt phosphorylation whereas it significantly induced phosphorylation of Erk1&2, resulting in an imbalance between the two signaling axes in vessels from non-diabetic (Fig. 5, A to C) and diabetic (Fig. 5, D to F) patients. Aortic rings from healthy wild-type mice were used as a positive control, confirming that insulin significantly induces Akt phosphorylation much more so than Erk1&2 in the vessel wall of these mice (Fig. 5, G to I). In line with our previous findings, insulin increased the phosphorylation of Akt, but not Erk1&2, in vascular segments from patients with diabetes taking oral DPP4i treatment (Fig. 5, J to L). These results confirm that there is a selective dysregulation of downstream insulin signaling in vessels from patients with vascular disease, in favor of Erk1&2 activation (over Akt), indicating the presence of vascular IR. This abnormal vascular insulin signaling can be reversed by pre-treatment with a DPP4i.

### **Characterizing the insulin-sensitizing properties of DPP4 inhibition**

To understand the mechanisms by which DPP4 inhibition regulates downstream insulin and redox signaling in the vascular wall of patients with atherosclerosis, we first examined whether DPP4 inhibition acts directly on the human vascular wall. Indeed, in the presence of a synthetic DPP4i, insulin increased the activation of Akt over Erk1&2 in both human arteries (Fig. 6, A to C) and veins (Fig. 6, D to F; fig. S13). To prove that this DPP4i-induced shift of insulin signaling in human vessels is responsible for the beneficial effect of the combined DPP4i/insulin treatment on vascular redox state, we first examined whether insulin activates Rac1 in the presence of an Erk1&2 inhibitor. We found that Erk1&2 inhibition by using 3-(2-Aminoethyl)-5-((4-ethoxyphenyl)methylene)-2,4-thiazolidinedione (Erk-i) abolished the ability of insulin to stimulate Rac1 GTP-activation, suggesting that Erk1&2 signaling is responsible for the insulin-mediated activation of NADPH-oxidases in human vascular disease

(Fig. 6G). On the contrary, the combination of insulin with DPP4i did not induce vascular eNOS phosphorylation in the presence of the Akt inhibitor wortmannin (Fig. 6H), suggesting that the DPP4i-induced effect of insulin on eNOS phosphorylation is dependent upon activation of Akt.

Insulin receptor substrate (IRS1) acts as a hub for insulin's signaling and its phosphorylation at Ser307 shifts post-receptor signaling towards Erk1&2. We examined whether DPP4 inhibition modifies the responses of human vessels to insulin by targeting IRS1. Indeed, DPP4i significantly reduced the phosphorylation of IRS1 at Ser307 (Fig. 6I). To understand how DPP4 inhibition controls IRS1 phosphorylation, we then explored the ability of DPP4i to regulate the activation of AMP-activate kinase (AMPK $\alpha$ 2), a molecule with known insulin-sensitizing properties, which has recently been linked with DPP4 signaling in in vitro models (16). We found that DPP4i directly induced phosphorylation of AMPK $\alpha$ 2 at its activation site Thr172 (Fig. 6J). Pre-incubation of human vessels with compound C, an AMPK inhibitor, rendered DPP4i unable to reverse the stimulatory effects of insulin on vascular NADPH-oxidase activity (Fig. 6K). Finally, AMPK inhibition abolished the ability of DPP4i to rescue insulin sensitivity (Fig. 6L). These findings suggest that DPP4i restores vascular insulin sensitivity and elicits antioxidant responses to insulin via an AMPK-mediated mechanism.

We further explored whether DPP4i exerts its insulin sensitizing effects by increasing the vascular bioavailability of GLP1. In the presence of GLP1R blockade, insulin still induced O<sub>2</sub><sup>-</sup> generation in human arteries, and DPP4i prevented this effect; however, DPP4i failed to lead to an insulin-induced reduction of vascular O<sub>2</sub><sup>-</sup> below the baseline, suggesting that abnormal insulin signaling in the vascular wall is not totally reversed by DPP4i in the presence of GLP1R blockade. This finding demonstrates that the effect of DPP4i on vascular insulin signaling is partly GLP1R-mediated (fig. S14, A to C). Considering that protein kinase C beta (PKC $\beta$ ) has demonstrated endothelial insulin-sensitising properties (17), we investigated whether PKC $\beta$

could drive the vascular effects of DPP4i. Upon PKC $\beta$  specific inhibition, we observed that the O<sub>2</sub><sup>-</sup>-propagating effects of insulin were attenuated (fig. S14, D to F). DPP4i, on the other hand, maintained its ability to further improve insulin sensitivity, as evidenced by the significant reduction in arterial O<sub>2</sub><sup>-</sup> in response to insulin, even in the presence of PKC $\beta$  inhibition (fig. S14, D to F).

We then explored the ability of DPP4i to modify redox-sensitive inflammatory transcriptional pathways in human primary endothelial cells. Indeed, DPP4i partly prevented nuclear translocation of nuclear factor kappa B (NFkB) in TNF- $\alpha$ -stimulated human umbilical vein endothelial cells (HUVEC) (fig. S15). Given that NFkB is a redox-sensitive transcriptional pathway, it is likely that it is directly involved in the development of vascular IR in human atherosclerosis.

### **Clinical implications of the interaction between DPP4 and insulin**

To explore the value of systemic DPP4 activity and insulin concentration as biomarkers of vascular redox state in patients with coronary artery disease, we stratified patients in subgroups depending on plasma DPP4 activity and insulin. We observed that patients in the lowest tertile of both DPP4 activity and insulin had markedly lower NADPH-oxidase-derived O<sub>2</sub><sup>-</sup> production in their IMA compared to patients in the highest tertile of DPP4 activity and insulin, as evaluated by measuring arterial NADPH-stimulated (Fig. 7A) and Vas2870-inhibitable (Fig. 7B) O<sub>2</sub><sup>-</sup> production, which was independent of the use of statins [known pleiotropic regulator of vascular NADPH-oxidases activity (18)] upon multivariate regression analysis (table S2). This confirmed a cumulative effect of high serum insulin and high DPP4 activity on vascular oxidative stress, introducing their potential role as combined biomarkers as well as therapeutic targets in patients with atherosclerosis.

Diabetes has an inflammatory pathophysiological component, and we have found that it is characterized by elevated plasma inflammatory cytokines such as interleukin 6 (IL6) and tumor necrosis factor alpha (TNF $\alpha$ ), as well as high sensitivity C-reactive protein (hsCRP). However, the circulating concentrations of these inflammatory biomarkers were not associated with arterial redox state (fig. S16), whereas the positive association of high DPP4 activity/high insulin with arterial NADPH-oxidases activity was independent of the circulating concentration of IL6, TNF $\alpha$ , or hsCRP (table S2).

We next explored the predictive value of DPP4 activity and insulin on cardiovascular and all-cause mortality. In total, we recorded 49 patient deaths, 21 of which classified as cardiac. Patients in the highest tertile for both serum DPP4 activity and serum insulin displayed significantly higher risk for cardiac death compared to the rest of the sample population (HR[95%CI]=3.431.02-11.54], P=0.047), after adjusting for traditional cardiovascular risk factors such as euroSCORE II, hyperlipidemia, hypertension, active smoking, NYHA class, and circulating hsCRP (as a marker of residual inflammatory risk) (Table 2, Fig. 7C).

## Discussion

This study demonstrates that the presence of vascular IR in humans with advanced atherosclerosis, independently of systemic IR or even diabetes, results in increased vascular oxidative stress and endothelial dysfunction when treated with human or synthetic insulins, independently of circulating plasma glucose. Importantly, this is reversed by DPP4 inhibition, which allows insulin to exert its antioxidant and vasoprotective actions, whereas the circulating DPP4/insulin balance is an independent predictor of cardiac mortality in patients with atherosclerosis (fig. S17).

Aggressive glycemic control has inconsistent effects on cardiovascular outcomes (19). The UKPDS trial first demonstrated that standard glycemic control (metformin vs sulfonylureas with/without insulin) reduced microvascular but not macrovascular disease risk (20). The ADVANCE trial further linked intensive glycemic control with reduced composite risk for vascular adverse events, which was, however, driven by reduced nephropathy risk (21), whereas the ACCORD trial showed no benefit of aggressive glycemic control on cardiovascular outcomes, suggesting the pharmacological means to achieve glycemic control may be as important as the degree of control (8). On the other hand, insulin treatment as a means of glycemic control has been associated with increased risk for acute ischemic events and cardiovascular (22) or all-cause mortality (23). The ORIGIN and DEVOTE trials also found no beneficial effect of insulin glargine or insulin degludec on cardiovascular risk (6, 7), highlighting the need to understand the direct effects of insulin on the vasculature.

Oxidative stress is a key feature of atherogenesis (24) and of vascular complications in diabetes and IR (4), and it has been proposed to play a role in endothelial IR (25). In vitro and animal studies have demonstrated that, under physiological conditions, insulin exerts antioxidant and vasodilatory effects via Akt-mediated increase in NO bioavailability in the vasculature (10, 26). On the other hand, endothelium-specific IR has been associated with endothelial dysfunction in mouse studies (27). Furthermore, hyperinsulinemia such as that observed in insulin-resistance states has been shown to cause endothelial dysfunction in vivo in humans, which was reversed by vitamin C, an antioxidant, suggesting an underlying role of oxidative stress in this effect of insulin (28). Our work strengthens this body of evidence by demonstrating that exogenous insulin treatment has a class effect characterized by NADPH-oxidase activation, eNOS uncoupling, endothelial dysfunction, and inflammatory pathway activation in human vessels from patients with atherosclerosis. This abnormal vascular response to insulin results from a default activation of Erk1&2 rather than Akt insulin

signalling in the human vascular cells of patients with atherosclerosis, which may compromise the vascular benefits of systemic serum glucose lowering. The association between cardiometabolic disease and resulting features of vascular IR was further confirmed in healthy versus HFD-fed ApoE<sup>-/-</sup> mice. The underlying causes may involve nutrient overload, low-grade inflammation or ageing and warrant further investigation.

We next explored the proof-of-concept that vascular insulin sensitization could reverse vascular insulin responses, as implied previously by the BARI 2D trial, where insulin-sensitizing approaches were associated with a favorable cardiovascular outcome in atherosclerosis patients (29). DPP4 is a glycoprotein that cleaves N-terminal dipeptides from proteins such as GLP1 (30), promoting IR in obesity and diabetes (31) whilst its pharmacological inhibition is a therapeutic target in diabetes and a potential insulin sensitizer (16). However, the vascular implications of DPP4i in humans and its interactions with vascular insulin signalling are unknown.

In this study we demonstrated that pre-treatment of patients with advanced atherosclerosis with an oral DPP4i *in vivo* as well as incubation of human vessels with DPP4i *ex vivo* reversed vascular responses to exogenous insulin treatment, resulting in an insulin-induced improvement of vascular redox state. This is due to the ability of DPP4i to reduce IRS1 Ser307 phosphorylation, which is known to regulate the switch between the two post-insulin receptor signalling pathways in *in vitro* and mouse models (16), in an AMPK $\alpha$ 2-mediated manner. Metformin, another insulin sensitizer that acts via AMPK signalling (15), did not have similar effects, which suggests that DPP4i may have more important pleiotropic effects via affecting GLP1R signalling as well as other pathways such as that of interleukin 10 (11).

Our work suggests that the effects of DPP4i are dependent on AMPK $\alpha$ 2, partly mediated by GLP1R signaling, but independent of PKC $\beta$  inhibition, another means of insulin sensitization

(17). We also show that, further to its short-term effects, DPP4i blocks proinflammatory NF $\kappa$ B signalling, which has been linked with molecular IR in endothelial cells (32), and this could have implications for chronic DPP4i treatment *in vivo*.

Clinical trials such as SAVOR-TIMI 53 and EXAMINE, have shown no benefit of DPP4i add-on antidiabetic treatment on cardiovascular complications of diabetes (33). On the other hand, a recent clinical trial showed that DPP4i administration on top of insulin treatment reduces the risk for stroke in patients with diabetes (34). In the recent CARMELINA trial examining the effect of linagliptin on cardiovascular outcomes, almost 60% of participants received insulin treatment (35). However, examining the interaction of DPP4i with insulin treatment in this case would be confounded because insulin was administered in cases where glycemic control was challenging as per clinical guidelines (thus being a surrogate of more advanced diabetes states than non-insulin-treated patients). Furthermore, significantly fewer patients in the linagliptin group initiated or increased doses of pre-existing insulin therapy (35), suggesting an inverse confounding association of insulin treatment and linagliptin treatment.

Our study has some potential limitations due to the nature of our clinical research population. Indeed, there are some borderline demographics differences between studies 1 and 2 and patients with or without diabetes within the studies which, although justified based on the individual study objectives, may introduce background statistical noise. However, we have applied careful statistical adjustments in our observational analyses and careful matching/paired design in our mechanistic experiments, which have been further validated in cell culture and animal models. In addition, there was a relatively small number of cardiac adverse events which is a limitation of the outcome arm of our study.

In conclusion, we show that IR is present in the vasculature of patients with coronary atherosclerosis even in the absence of diabetes or markers of systemic IR. This results in

vascular oxidative stress and endothelial dysfunction in response to insulin. Pharmacological treatment with DPP4 inhibitors restores “physiological” insulin signalling in human vessels, allowing insulin to improve vascular redox state and endothelial function. These results strengthen the proof-of-concept for the importance of vascular sensitization in diabetes and call for appropriately designed randomized clinical trials to explore the effect of combined treatment with insulin and DPP4-i on cardiovascular outcomes in patients with diabetes and atherosclerosis, which could help expand the clinical benefits associated with glycemic control.

## **Methods**

### **Study design**

In this study we explored the direct effects of insulin on vascular redox state and endothelial function in patients with atherosclerosis to understand why intensive glucose lowering fails to prevent the macrovascular effects of diabetes. We also investigated the ability of DPP4 inhibition to modify vascular insulin signalling in this population. In study 1 we used a cohort of 580 consecutively enrolled patients with advanced atherosclerosis, undergoing cardiac surgery, to explore the links between endogenous circulating insulin / plasma DPP4 activity and vascular redox signalling studied directly in human vessels obtained during surgery. We then explored the value of endogenous plasma insulin / DPP4 activity in predicting cardiac mortality during the 3.9 years prospective follow up period. In study 2, we further explored the mechanisms by which exogenous insulin treatment and DPP4 inhibition affect vascular redox signalling, by using *ex vivo* models of human vessels (arteries and veins obtained from 94 consecutively enrolled patients undergoing cardiac surgery), as described below. These models provide unique insights to the underlying mechanisms of vascular redox regulation in humans, despite inherent limitations of *in vivo* translation. The mechanisms behind the findings were

further explored using human primary endothelial cell culture and causality was tested in vivo with high fat diet (HFD)-fed ApoE<sup>-/-</sup> mice (treated with linagliptin vs vehicle followed by insulin stimulation)

Study 1 was powered against vascular superoxide in human mammary arteries. We estimated that we would need 161 patients to detect a 6% difference between the bottom and top tertiles of arterial Log(O<sub>2</sub><sup>-</sup>) with power 0.9 and Log(O<sub>2</sub><sup>-</sup>) SD of 0.36. Similarly, we would need 157 patients to detect a 13% difference between the top and bottom tertiles of Log(NADPH-stimulated O<sub>2</sub><sup>-</sup>) with power 0.9 and Log(NADPH-stimulated O<sub>2</sub><sup>-</sup>) SD of 0.71. In addition, 160 patients would be needed to detect a 21% difference in Log(Vas2870-inhibitable O<sub>2</sub><sup>-</sup>) between the bottom and top tertiles with power 0.9 and Log(Vas2870-inhibitable O<sub>2</sub><sup>-</sup>) SD of 0.69. For the outcome analysis, power calculations suggested that with 21 cardiac deaths in 580 patients during prospective follow-up, we would have power 0.8 to detect a hazard ratio of 3.3 with event probability of 0.07 and non-inferiority margin of 0.1

In Study 2, the ex vivo experiments were also powered against vascular O<sub>2</sub><sup>-</sup> generation. We estimated that with a minimum of 5 pairs of samples (serial rings from the same vessel) we would be able to identify a change of the desired readout in response to an intervention (i.e., a change in Log(O<sub>2</sub><sup>-</sup>)) by 0.48 with  $\alpha=0.05$ , power 0.9 and SD for a difference in the response of the pairs of 0.25. Similarly, with 5 patients per group we would be able to detect a 47% change in NADPH-stimulated O<sub>2</sub><sup>-</sup> and a 44% change in Vas2870-inhibitable O<sub>2</sub><sup>-</sup> with power 0.9 and  $\alpha=0.05$ . For the vasomotor studies, we estimated that with n=5 sets of serial rings, we would be able to detect 35% change in maximum vasorelaxation and 40% change in EC50, with power 0.9 and  $\alpha=0.05$ .

## Study population

Study 1 included 580 prospectively recruited patients undergoing elective cardiac surgery at the John Radcliffe hospital, Oxford University Hospitals NHS Trust. During surgery, SV and IMA segments were obtained and transferred to the lab within 20 minutes from harvesting, and used for superoxide ( $O_2^{\cdot-}$ ) measurements and vasomotor studies. Blood samples were also collected prior to surgery and processed within 20 minutes. Patients were followed-up for a mean of  $3.9 \pm 0.4$  years and mortality was recorded.

Study 2 included 94 patients undergoing CABG surgery at the John Radcliffe hospital, Oxford University Hospitals NHS Trust. Vascular segments and ThAT from the mediastinal region were collected and incubated with insulin with or without pre-incubation with a DPP4-i as explained in the *online supplemental material*. The incubated samples were then used for  $O_2^{\cdot-}$  measurements, vasomotor studies, western immunoblotting and other signalling experiments.

The demographic characteristics of study 1 and 2 participants can be found in Table 1 and table S1. Study 2 had higher prevalence of diabetes and hypercholesterolaemia, since it was specifically designed to allow comparison of the responsiveness of human vessels from patients with and without diabetes to the study interventions, unlike study arm 1 that included unselected, consecutive patients undergoing coronary bypass surgery. The use of human vessels from patients with atherosclerosis with multiple risk factors, taking standard medication for stable CAD, is a strength of this work, as any finding is directly translatable to the typical patient with atherosclerosis.

Participants in any of the two studies should satisfy all of the following inclusion criteria: i) ability to give informed consent for participation in the study and willingness to comply with all study requirements; ii) male or female volunteers, aged 18 years or above; iii) patients undergoing cardiac surgery. Exclusion criteria included any inflammatory (idiopathic or

autoimmune) or infective disease (viral or bacterial disease), renal failure (on dialysis) or liver failure, active malignancy, active use of non-steroidal or anti-inflammatory drugs and any other significant disease or disorder which, in the opinion of the Investigator, may either put the volunteer at risk because of participation in the study, or may influence the result of the study, or the volunteer's ability to participate in the study. The protocols of the studies complied with the Declaration of Helsinki, and all patients provided informed written consent.

### **Follow-up for clinical outcomes**

All patients were prospectively recruited in the Oxford Heart Vessels and Fat (ox-HVF) cohort that collects mortality and outcome data by linking the Office for National Statistics (ONS) data with National Health Service (NHS) Digital, a nation-wide service that collects all data from the electronic patient records available in every NHS hospital in England. Patients had provided consent and the collected data was first stored in a secured network and then link-anonymized and analysed. Events were recorded by the clinical care team, being the formal diagnosis for hospitalization or formal primary cause of death, given by the respective NHS hospitals for every hospital admission or outpatient visit. NHS digital is also connected with the UK Office for National Statistics, which offers further cross-check of the mortality data and cause of death. Patients were followed-up after surgery until the date of NHS Digital data collection or death. Right-censoring was applied for patients that were alive at the data collection time. Follow-up time was defined as the number of days between surgery and the date of data collection (December 15, 2017) or date of death. Adjudication of the cause of death was defined by 3 independent study investigators in a blinded way, based on the International Statistical Classification of Diseases and Related Health Problems 10th Revision (ICD-10) codes. Cardiac mortality was defined as any death due to proximate cardiac causes (chronic

ischemic heart disease), corresponding to ICD-10 codes of I20-I25 (ischemic heart diseases) and I30-53 (other forms of heart disease) (36).

### **Risk factor definition**

Traditional cardiovascular risk factors were defined according to clinical guidelines and following an interview with each study participant and careful review of their medical notes. Hypertension was defined based on the presence of a documented diagnosis or treatment with an antihypertensive regimen (37). Similar criteria were used for the definition of hypercholesterolemia and diabetes mellitus (38, 39). Smoking history was also assessed, and patients were grouped as never-smokers, ex-smokers (quit >1 week ago) or active smokers.

### **Mice**

Wild-type C57BL/6 mice (strain C57BL/6, ENVIGO labs, UK) were used for aortic tissue ex vivo insulin incubations as biological atherosclerosis-free controls. To test the in vivo ability of DPP4i to regulate vascular insulin responses in the context of cardiometabolic disease, adult (8-10 weeks) male C57BL6/ApoE<sup>-/-</sup> mice were fed a HFD (SDS829108 Western RD diet) and treated with either linagliptin (a DPP4i, Cayman Chemicals; 10mg/kg in 0.5% carboxymethyl cellulose in sterile distilled water) or control (0.5% carboxymethyl cellulose in sterile distilled water) by oral gavage once daily (between 9-10am) for 28 days. Previous animal and human in vivo studies have established that DPP4 inhibitors successfully reduce abnormally high glucose without inducing hypoglycemia, hence continuous glucose monitoring of the circulating glucose levels was not performed. Mice were then culled by exsanguination under terminal anaesthetic (isoflurane >4% in 95% O<sub>2</sub>/5% CO<sub>2</sub>), where depth of anaesthesia was monitored by respiration rate and withdrawal reflexes. Aortic tissue was harvested and used

for measuring vascular  $O_2^-$  and its sources, as well as for vasomotor myograph studies after ex vivo insulin incubations.

All animal studies were conducted with ethical approval from the Local Ethical Review Committee and in accordance with the UK Home Office regulations (Guidance on the Operation of Animals, Scientific Procedures Act, 1986) and were approved by the Local Ethical Review Committee. Mice were housed in a specific pathogen-free environment, in Tecniplast Sealsafe IVC cages (floor area 542 cm<sup>2</sup>) with a maximum of six other mice. Mice were kept in a 12 h light/dark cycle and in controlled temperatures (20–22°C). Water and food were available *ad libitum*.

### **Blood sampling and circulating biomarker measurements**

Venous blood was collected prior to surgery after 8h of fasting and serum or plasma was isolated by centrifugation at 3,000g for 15min at 4°C. Serum glucose, insulin and plasma hsCRP were measured as described previously (40). Homeostatic model assessment of systemic IR (HOMA-IR) was calculated by the formula (glucose x insulin)/405 (glucose measured in mg/dL and insulin in mU/L). Serum DPP4 activity was measured by a commercial kit (Biovision) according to the manufacturer's instructions. Serum IL6 and TNF $\alpha$  were measured by the Quantikine HS ELISA Human IL-6 Immunoassay (order ID: HS600C) and Quantikine HS ELISA Human TNF $\alpha$  Immunoassay (order ID: HSTA00E) from R&D Systems Europe, Ltd., according to the manufacturer's instructions.

### **Transcriptomic profiling of human vessels**

The comprehensive measurement of protein coding and long intergenic non-coding RNA transcripts in patients' samples was performed using the Human Gene-2.1 ST Array and the GeneTitan System (Affymetrix). Microarray data analyses and identification of the differentially expressed genes were performed using the GeneChip Expression Analysis Software (version 4, Affymetrix). Pathway enrichment analysis was carried out in ConsensusPathDB-human (<http://cpdb.molgen.mpg.de/>).

### **Statistical analysis**

Study 1 is a prospective cohort study (the Oxford Heart Vessels and Fat Cohort or ox-HVF cohort, see [www.oxhvf.com](http://www.oxhvf.com)) of consecutive patients undergoing cardiac surgery, used to test associations between endogenous insulin/DPP4 activity and parameters of vascular function. Study 2 was a mechanistic study involving cases where vascular tissue samples were harvested and used for mechanistic ex vivo experiments. The ex vivo effects of insulin and other interventions on vascular function were tested in serial vascular rings from the same patients, leading to reduced background variability and need for fewer patients in each individual experiment due to the paired design. This cohort was enriched for T2DM patients to allow for safe mechanistic conclusions which were consistent in both patients with and without diabetes, and this is a strength of study 2. Continuous variables were tested for normal distribution using the Kolmogorov-Smirnov test. Non-normally distributed variables were log-transformed for analysis.

In the clinical studies, continuous variables between 3 groups were compared by using one-way ANOVA followed by Bonferoni post-hoc test for individual comparisons. For the organ bath experiments, the effect of “serum insulin tertile” on vasorelaxations in response to ACh

& BK was evaluated by using two-way ANOVA for repeated measures (examining the effect of “Ach, BK or SNP concentration” x “serum insulin tertile” interaction on “vasorelaxations”), in a full factorial model.

Sample size calculations were based on previous data from our laboratory. For the *ex vivo* experiments, sample size calculations were performed based on our previous experience on this model (18), and we estimated that with a minimum of 5 pairs of samples (serial rings from the same vessel) we would be able to identify a change of  $\log(\text{O}_2^-)$  by 0.48 with  $\alpha=0.05$ , power 0.9 and SD for a difference in the response of the pairs of 0.25. Furthermore,  $n = 5$  sets of independent experiments is also supported by recent guidelines for biological experiments (43). Analysis of paired *ex vivo* mechanistic experiments was performed by Wilcoxon’s sign rank tests, while Bonferroni post-hoc corrections for individual comparisons were employed as appropriate. For the *ex vivo* organ bath experiments using serial rings from the same vessel incubated with multiple interventions, we performed repeated measures ANOVA and paired t-tests for individual comparisons, followed by Bonferroni post-hoc correction for multiple testing as appropriate.

To test the cumulative association of serum DPP4 activity and serum insulin with mortality rates, we created dichotomous categorical variable by splitting the population of Study 1 into two groups, one with patients in the high tertile for both serum DPP4 activity and serum insulin and one in the intermediate/low tertiles for those two biomarkers. The combined effect of serum insulin and DPP4 activity on all-cause and cardiac mortality was then examined by multivariate Cox regression survival analysis after adjusting for all traditional cardiovascular risk factors (euroSCORE II, hyperlipidaemia, hypertension, active smoking) and plasma hsCRP). We only corrected for risk factors and not the medication associated with them, in order to avoid overfitting collinearity errors, as per standard practice in this type of clinical studies.

With regards to microarray data processing, normalisation, quality control and differential gene expression analysis was performed with the Affymetrix Transcriptome Analysis Console (TAC 4.0) Software. The statistical comparisons between treatments was done following a repeated measures model for the individual patients. Insulin pathway enrichment analysis was carried out in ConsensusPathDB-human with differentially expressed genes (DEGs) (Insulin-treated vs. untreated-controls) that displayed fold change (linear) $>1$  or  $<-1$  and a p-value  $< 0.05$ . Gene Ontology database was used to functionally annotate DEGs. Raw data are provided in data file S1.

## **Supplementary materials and methods list**

### Supplementary Methods

Fig. S1. Direct effects of human insulin and insulin analogues on endothelial function ex vivo in humans

Fig. S2. Association between serum insulin and NADPH-oxidases activity in humans

Fig. S3. Dose-response effects of human insulin and insulin analogues on human vascular redox state

Fig. S4. Effects of human insulin on vascular redox state in humans

Fig. S5. Effects of insulin on proinflammatory transcriptional pathways in human arteries

Fig. S6. Effects of human insulin on vascular redox state in wild-type mice

Fig. S7. Effects of insulin on vascular redox state in patients with diabetes on metformin

Fig. S8. Dipeptidyl peptidase 4 inhibition (DPP4i) regulates the effects of human insulin on human vascular redox state

Fig. S9. Dipeptidyl peptidase 4 inhibition has no direct superoxide ( $O_2^{\cdot-}$ )-scavenging properties

Fig. S10. Linagliptin, a dipeptidyl peptidase 4 inhibitor, reverses the pro-oxidant effects of insulin on the vasculature of high fat diet (HFD)-fed ApoE<sup>-/-</sup> mice

Fig. S11. Association between circulating DPP4 activity and vascular redox state in humans

Fig. S12. Linagliptin reverses the effect of insulin on endothelial function in high fat diet (HFD)-fed ApoE<sup>-/-</sup> mice

Fig. S13. Dipeptidyl peptidase 4 inhibition (DPP4i) regulates the downstream signalling balance in response to human insulin in humans

Fig. S14. The role of glucagon like peptide 1 receptor (GLP1R) and protein kinase C $\beta$  (PKC $\beta$ ) signalling in the vascular insulin-sensitizing properties of dipeptidyl peptidase 4 inhibition (DPP4i)

Fig. S15. Effect of dipeptidyl peptidase 4 inhibition on nuclear factor kappa beta (NF $\kappa$ B) nuclear translocation

Fig. S16. Proinflammatory cytokines, diabetes and arterial redox state in humans with atherosclerosis

fig. S17. Summary and proposed mechanism

Table S1. Demographic characteristics of patients with and without diabetes

Table S2. Multivariate regression analysis testing the interaction between Insulin/DPP4 activity, use of statins, and plasma inflammatory biomarkers in predicting Vas2870-inhibitable superoxide ( $O_2^{\cdot-}$ ) in human internal mammary arteries (IMA)

Data file S1. Raw data

## References

1. F. Paneni, J. A. Beckman, M. A. Creager, F. Cosentino, Diabetes and vascular disease: pathophysiology, clinical consequences, and medical therapy: part I. *Eur Heart J* **34**, 2436-2443 (2013).
2. I. Akoumianakis, C. Antoniades, Impaired Vascular Redox Signaling in the Vascular Complications of Obesity and Diabetes Mellitus. *Antioxid Redox Signal* **30**, 333-353 (2019).
3. J. Shi, S. Wu, C. L. Dai, Y. Li, I. Grundke-Iqbal, K. Iqbal, F. Liu, C. X. Gong, Diverse regulation of AKT and GSK-3 $\beta$  by O-GlcNAcylation in various types of cells. *FEBS Lett* **586**, 2443-2450 (2012).
4. I. Akoumianakis, C. Antoniades, Impaired Vascular Redox Signaling in the Vascular Complications of Obesity and Diabetes Mellitus. *Antioxid Redox Signal*, (2018).
5. E. Mannucci, S. Giannini, I. Dicembrini, Cardiovascular effects of basal insulins. *Drug Healthc Patient Saf* **7**, 113-120 (2015).
6. O. T. Investigators, H. C. Gerstein, J. Bosch, G. R. Dagenais, R. Diaz, H. Jung, A. P. Maggioni, J. Pogue, J. Probstfield, A. Ramachandran, M. C. Riddle, L. E. Ryden, S. Yusuf, Basal insulin and cardiovascular and other outcomes in dysglycemia. *N Engl J Med* **367**, 319-328 (2012).
7. S. P. Marso, D. K. McGuire, B. Zinman, N. R. Poulter, S. S. Emerson, T. R. Pieber, R. E. Pratley, P. M. Haahr, M. Lange, K. Brown-Frandsen, A. Moses, S. Skibsted, K. Kvist, J. B. Buse, D. S. Group, Efficacy and Safety of Degludec versus Glargine in Type 2 Diabetes. *N Engl J Med* **377**, 723-732 (2017).
8. G. Action to Control Cardiovascular Risk in Diabetes Study, H. C. Gerstein, M. E. Miller, R. P. Byington, D. C. Goff, Jr., J. T. Bigger, J. B. Buse, W. C. Cushman, S. Genuth, F. Ismail-Beigi, R. H. Grimm, Jr., J. L. Probstfield, D. G. Simons-Morton, W. T. Friedewald, Effects of intensive glucose lowering in type 2 diabetes. *N Engl J Med* **358**, 2545-2559 (2008).
9. J. M. Lizcano, D. R. Alessi, The insulin signalling pathway. *Curr Biol* **12**, R236-238 (2002).
10. M. Montagnani, H. Chen, V. A. Barr, M. J. Quon, Insulin-stimulated activation of eNOS is independent of Ca<sup>2+</sup> but requires phosphorylation by Akt at Ser(1179). *J Biol Chem* **276**, 30392-30398 (2001).
11. G. P. Fadini, A. Avogaro, Cardiovascular effects of DPP-4 inhibition: beyond GLP-1. *Vascul Pharmacol* **55**, 10-16 (2011).
12. S. C. Gough, S. Harris, V. Woo, M. Davies, Insulin degludec: overview of a novel ultra long-acting basal insulin. *Diabetes Obes Metab* **15**, 301-309 (2013).
13. W. E. Owen, W. L. Roberts, Cross-reactivity of three recombinant insulin analogs with five commercial insulin immunoassays. *Clin Chem* **50**, 257-259 (2004).
14. K. McKeage, K. L. Goa, Insulin glargine: a review of its therapeutic use as a long-acting agent for the management of type 1 and 2 diabetes mellitus. *Drugs* **61**, 1599-1624 (2001).
15. C. R. Triggle, H. Ding, Metformin is not just an antihyperglycaemic drug but also has protective effects on the vascular endothelium. *Acta Physiol (Oxf)* **219**, 138-151 (2017).
16. E. Kornelius, C. L. Lin, H. H. Chang, H. H. Li, W. N. Huang, Y. S. Yang, Y. L. Lu, C. H. Peng, C. N. Huang, DPP-4 Inhibitor Linagliptin Attenuates Abeta-induced Cytotoxicity through Activation of AMPK in Neuronal Cells. *CNS Neurosci Ther* **21**, 549-557 (2015).
17. C. E. Tabit, S. M. Shenouda, M. Holbrook, J. L. Fetterman, S. Kiani, A. A. Frame, M. A. Kluge, A. Held, M. M. Dohadwala, N. Gokce, M. G. Farb, J. Rosenzweig, N. Ruderman, J. A. Vita, N. M. Hamburg, Protein kinase C- $\beta$  contributes to impaired endothelial insulin signaling in humans with diabetes mellitus. *Circulation* **127**, 86-95 (2013).
18. C. Antoniades, C. Bakogiannis, P. Leeson, T. J. Guzik, M. H. Zhang, D. Tousoulis, A. S. Antonopoulos, M. Demosthenous, K. Marinou, A. Hale, A. Paschalis, C. Psarros, C. Triantafyllou, J. Bendall, B. Casadei, C. Stefanadis, K. M. Channon, Rapid, direct effects of statin treatment on arterial redox state and nitric oxide bioavailability in human atherosclerosis via

- tetrahydrobiopterin-mediated endothelial nitric oxide synthase coupling. *Circulation* **124**, 335-345 (2011).
19. G. Dailey, E. Wang, A review of cardiovascular outcomes in the treatment of people with type 2 diabetes. *Diabetes Ther* **5**, 385-402 (2014).
  20. Intensive blood-glucose control with sulphonylureas or insulin compared with conventional treatment and risk of complications in patients with type 2 diabetes (UKPDS 33). UK Prospective Diabetes Study (UKPDS) Group. *Lancet* **352**, 837-853 (1998).
  21. A. C. Group, A. Patel, S. MacMahon, J. Chalmers, B. Neal, L. Billot, M. Woodward, M. Marre, M. Cooper, P. Glasziou, D. Grobbee, P. Hamet, S. Harrap, S. Heller, L. Liu, G. Mancia, C. E. Mogensen, C. Pan, N. Poulter, A. Rodgers, B. Williams, S. Bompont, B. E. de Galan, R. Joshi, F. Travert, Intensive blood glucose control and vascular outcomes in patients with type 2 diabetes. *N Engl J Med* **358**, 2560-2572 (2008).
  22. C. L. Rounie, R. A. Greevy, C. G. Grijalva, A. M. Hung, X. Liu, H. J. Murff, T. A. Elasy, M. R. Griffin, Association between intensification of metformin treatment with insulin vs sulfonylureas and cardiovascular events and all-cause mortality among patients with diabetes. *JAMA* **311**, 2288-2296 (2014).
  23. L. N. McEwen, A. J. Karter, B. E. Waitzfelder, J. C. Crosson, D. G. Marrero, C. M. Mangione, W. H. Herman, Predictors of mortality over 8 years in type 2 diabetic patients: Translating Research Into Action for Diabetes (TRIAD). *Diabetes Care* **35**, 1301-1309 (2012).
  24. I. Akoumianakis, C. Antoniadis, The interplay between adipose tissue and the cardiovascular system: is fat always bad? *Cardiovasc Res* **113**, 999-1008 (2017).
  25. F. Paneni, S. Costantino, F. Cosentino, Role of oxidative stress in endothelial insulin resistance. *World J Diabetes* **6**, 326-332 (2015).
  26. M. A. Potenza, F. Addabbo, M. Montagnani, Vascular actions of insulin with implications for endothelial dysfunction. *Am J Physiol Endocrinol Metab* **297**, E568-577 (2009).
  27. M. T. Kearney, Changing the way we think about endothelial cell insulin sensitivity, nitric oxide, and the pathophysiology of type 2 diabetes: the FoxO is loose. *Diabetes* **62**, 1386-1388 (2013).
  28. G. Arcaro, A. Cretti, S. Balzano, A. Lechi, M. Muggeo, E. Bonora, R. C. Bonadonna, Insulin causes endothelial dysfunction in humans: sites and mechanisms. *Circulation* **105**, 576-582 (2002).
  29. B. D. S. Group, R. L. Frye, P. August, M. M. Brooks, R. M. Hardison, S. F. Kelsey, J. M. MacGregor, T. J. Orchard, B. R. Chaitman, S. M. Genuth, S. H. Goldberg, M. A. Hlatky, T. L. Jones, M. E. Molitch, R. W. Nesto, E. Y. Sako, B. E. Sobel, A randomized trial of therapies for type 2 diabetes and coronary artery disease. *N Engl J Med* **360**, 2503-2515 (2009).
  30. N. H. Kim, T. Yu, D. H. Lee, The nonglycemic actions of dipeptidyl peptidase-4 inhibitors. *Biomed Res Int* **2014**, 368703 (2014).
  31. D. Lamers, S. Famulla, N. Wronkowitz, S. Hartwig, S. Lehr, D. M. Ouwens, K. Eckardt, J. M. Kaufman, M. Ryden, S. Muller, F. G. Hanisch, J. Ruige, P. Arner, H. Sell, J. Eckel, Dipeptidyl peptidase 4 is a novel adipokine potentially linking obesity to the metabolic syndrome. *Diabetes* **60**, 1917-1925 (2011).
  32. Y. Hasegawa, T. Saito, T. Ogihara, Y. Ishigaki, T. Yamada, J. Imai, K. Uno, J. Gao, K. Kaneko, T. Shimosawa, T. Asano, T. Fujita, Y. Oka, H. Katagiri, Blockade of the nuclear factor-kappaB pathway in the endothelium prevents insulin resistance and prolongs life spans. *Circulation* **125**, 1122-1133 (2012).
  33. E. Mannucci, O. Mosenzon, A. Avogaro, Analyses of Results From Cardiovascular Safety Trials With DPP-4 Inhibitors: Cardiovascular Outcomes, Predefined Safety Outcomes, and Pooled Analysis and Meta-analysis. *Diabetes Care* **39 Suppl 2**, S196-204 (2016).
  34. F. S. Yen, J. H. Chiang, C. W. Pan, B. J. Lin, J. C. Wei, C. C. Hsu, Cardiovascular outcomes of dipeptidyl peptidase-4 inhibitors in patients with type 2 diabetes on insulin therapy. *Diabetes Res Clin Pract* **140**, 279-287 (2018).
  35. J. Rosenstock, V. Perkovic, O. E. Johansen, M. E. Cooper, S. E. Kahn, N. Marx, J. H. Alexander, M. Pencina, R. D. Toto, C. Wanner, B. Zinman, H. J. Woerle, D. Baanstra, E. Pfarr, S. Schnaidt,

- T. Meinicke, J. T. George, M. von Eynatten, D. K. McGuire, C. Investigators, Effect of Linagliptin vs Placebo on Major Cardiovascular Events in Adults With Type 2 Diabetes and High Cardiovascular and Renal Risk: The CARMELINA Randomized Clinical Trial. *JAMA* **321**, 69-79 (2019).
36. K. A. Hicks, J. E. Tcheng, B. Bozkurt, B. R. Chaitman, D. E. Cutlip, A. Farb, G. C. Fonarow, J. P. Jacobs, M. R. Jaff, J. H. Lichtman, M. C. Limacher, K. W. Mahaffey, R. Mehran, S. E. Nissen, E. E. Smith, S. L. Targum, 2014 ACC/AHA Key Data Elements and Definitions for Cardiovascular Endpoint Events in Clinical Trials: A Report of the American College of Cardiology/American Heart Association Task Force on Clinical Data Standards (Writing Committee to Develop Cardiovascular Endpoints Data Standards). *J Am Coll Cardiol* **66**, 403-469 (2015).
  37. P. A. James, S. Oparil, B. L. Carter, W. C.ushman, C. Dennison-Himmelfarb, J. Handler, D. T. Lackland, M. L. LeFevre, T. D. MacKenzie, O. Ogedegbe, S. C. Smith, Jr., L. P. Svetkey, S. J. Taler, R. R. Townsend, J. T. Wright, Jr., A. S. Narva, E. Ortiz, 2014 evidence-based guideline for the management of high blood pressure in adults: report from the panel members appointed to the Eighth Joint National Committee (JNC 8). *JAMA* **311**, 507-520 (2014).
  38. A. American Diabetes, Diagnosis and classification of diabetes mellitus. *Diabetes Care* **37 Suppl 1**, S81-90 (2014).
  39. N. J. Stone, J. G. Robinson, A. H. Lichtenstein, C. N. Bairey Merz, C. B. Blum, R. H. Eckel, A. C. Goldberg, D. Gordon, D. Levy, D. M. Lloyd-Jones, P. McBride, J. S. Schwartz, S. T. Shero, S. C. Smith, Jr., K. Watson, P. W. Wilson, G. American College of Cardiology/American Heart Association Task Force on Practice, 2013 ACC/AHA guideline on the treatment of blood cholesterol to reduce atherosclerotic cardiovascular risk in adults: a report of the American College of Cardiology/American Heart Association Task Force on Practice Guidelines. *J Am Coll Cardiol* **63**, 2889-2934 (2014).
  40. A. S. Antonopoulos, M. Margaritis, P. Coutinho, C. Shirodaria, C. Psarros, L. Herdman, F. Sanna, R. De Silva, M. Petrou, R. Sayeed, G. Krasopoulos, R. Lee, J. Digby, S. Reilly, C. Bakogiannis, D. Tousoulis, B. Kessler, B. Casadei, K. M. Channon, C. Antoniades, Adiponectin as a link between type 2 diabetes and vascular NADPH oxidase activity in the human arterial wall: the regulatory role of perivascular adipose tissue. *Diabetes* **64**, 2207-2219 (2015).
  41. C. Antoniades, C. Shirodaria, N. Warrick, S. Cai, J. de Bono, J. Lee, P. Leeson, S. Neubauer, C. Ratnatunga, R. Pillai, H. Refsum, K. M. Channon, 5-methyltetrahydrofolate rapidly improves endothelial function and decreases superoxide production in human vessels: effects on vascular tetrahydrobiopterin availability and endothelial nitric oxide synthase coupling. *Circulation* **114**, 1193-1201 (2006).
  42. M. Margaritis, A. S. Antonopoulos, J. Digby, R. Lee, S. Reilly, P. Coutinho, C. Shirodaria, R. Sayeed, M. Petrou, R. De Silva, S. Jalilzadeh, M. Demosthenous, C. Bakogiannis, D. Tousoulis, C. Stefanadis, R. P. Choudhury, B. Casadei, K. M. Channon, C. Antoniades, Interactions between vascular wall and perivascular adipose tissue reveal novel roles for adiponectin in the regulation of endothelial nitric oxide synthase function in human vessels. *Circulation* **127**, 2209-2221 (2013).
  43. M. J. Curtis, S. Alexander, G. Cirino, J. R. Docherty, C. H. George, M. A. Gienbycz, D. Hoyer, P. A. Insel, A. A. Izzo, Y. Ji, D. J. MacEwan, C. G. Sobey, S. C. Stanford, M. M. Teixeira, S. Wonnacott, A. Ahluwalia, Experimental design and analysis and their reporting II: updated and simplified guidance for authors and peer reviewers. *Br J Pharmacol* **175**, 987-993 (2018).

**Funding:** This study was funded by Sanofi Aventis Deutschland GmbH, the British Heart Foundation (FS/16/15/32047 and Oxford British Heart Foundation Centre of Research Excellence), the National Institute for Health Research (NIHR) and the Oxford Biomedical Research Centre (BRC). IA acknowledges funding support by the Alexandros S Onassis Public Benefit Foundation.

**Author contributions:** I.A. conceived and performed experiments, performed data collection and analysis and wrote the manuscript. I.B. performed experiments. G.D. performed experiments. S.C. performed experiments. L.H. contributed to patient recruitment and data analysis. N.A. contributed to data analysis. M.M. contributed to data collection and analysis. A.S.A. contributed to patient recruitment and data analysis. E.K.O. contributed to data analysis. C.P. contributed to data analysis. N.G. contributed to data analysis. D.T. reviewed the manuscript. A.K. contributed to manuscript review. R.S. contributed to surgical specimen collection. G.K. contributed to surgical specimen collection. M.P. contributed to surgical specimen collection. U.S. performed experiments. P.W. provided scientific expertise and experimental design support. N.T. provided scientific expertise and experimental design support. K.M.C. was involved in the design of the study secured funding and provided scientific support. C.A. conceived the study, secured funding and reviewed the manuscript.

**Competing interests:** This study has been funded by Sanofi Aventis. C.A and K.M.C. are founders, shareholders and directors of Caristo Diagnostics, an image analysis company.

**Data and materials availability:** All data associated with this study are present in the paper or supplementary materials. The microarray data are accessible on a public depository (accession number GSE147598, which can be found on the following link: <https://www.ncbi.nlm.nih.gov/geo/query/acc.cgi?acc=GSE147598>).

## Figures

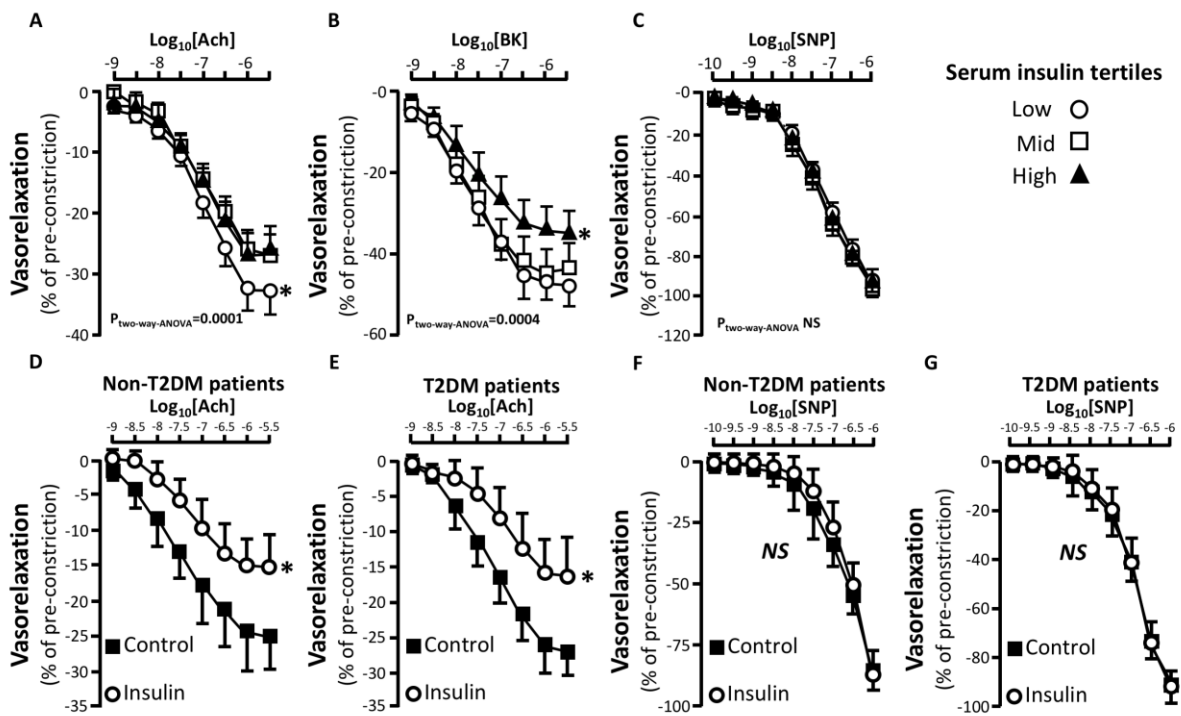


**Fig. 1. Insulin impairs endothelial function in humans with coronary atherosclerosis.**

(A-C) Vasorelaxation curves of phenylephrine pre-contracted human vessels in response to (A) acetylcholine (Ach, endothelium-dependent,  $n = 110$ ), (B) bradykinin (BK, endothelium-dependent,  $n = 38$ ), and (C) sodium nitroprusside (SNP, endothelium-independent,  $n = 92$ ) per circulating insulin tertiles in study arm 1. (D-E) Serial rings of human vessels were treated with and without insulin M1 ( $10 \mu\text{M}$ ) prior to testing vasorelaxation in response to acetylcholine [D for patients without diabetes ( $n=6$  pairs) and E for patients with diabetes ( $n=6$  pairs)] or sodium nitroprusside-SNP [F for patients without diabetes ( $n=6$  pairs) and G for patients with diabetes ( $n=6$  pairs)]. \* $P < 0.05$  vs high tertile in panel A; vs low tertile in panel B; vs control in panels D-E; NS: non-significant vs control ( $P > 0.05$ );  $P$ -values calculated by two-way ANOVA for repeated measures with (Ach dose)  $\times$  (insulin treatment) interaction; data presented as mean  $\pm$  SEM.

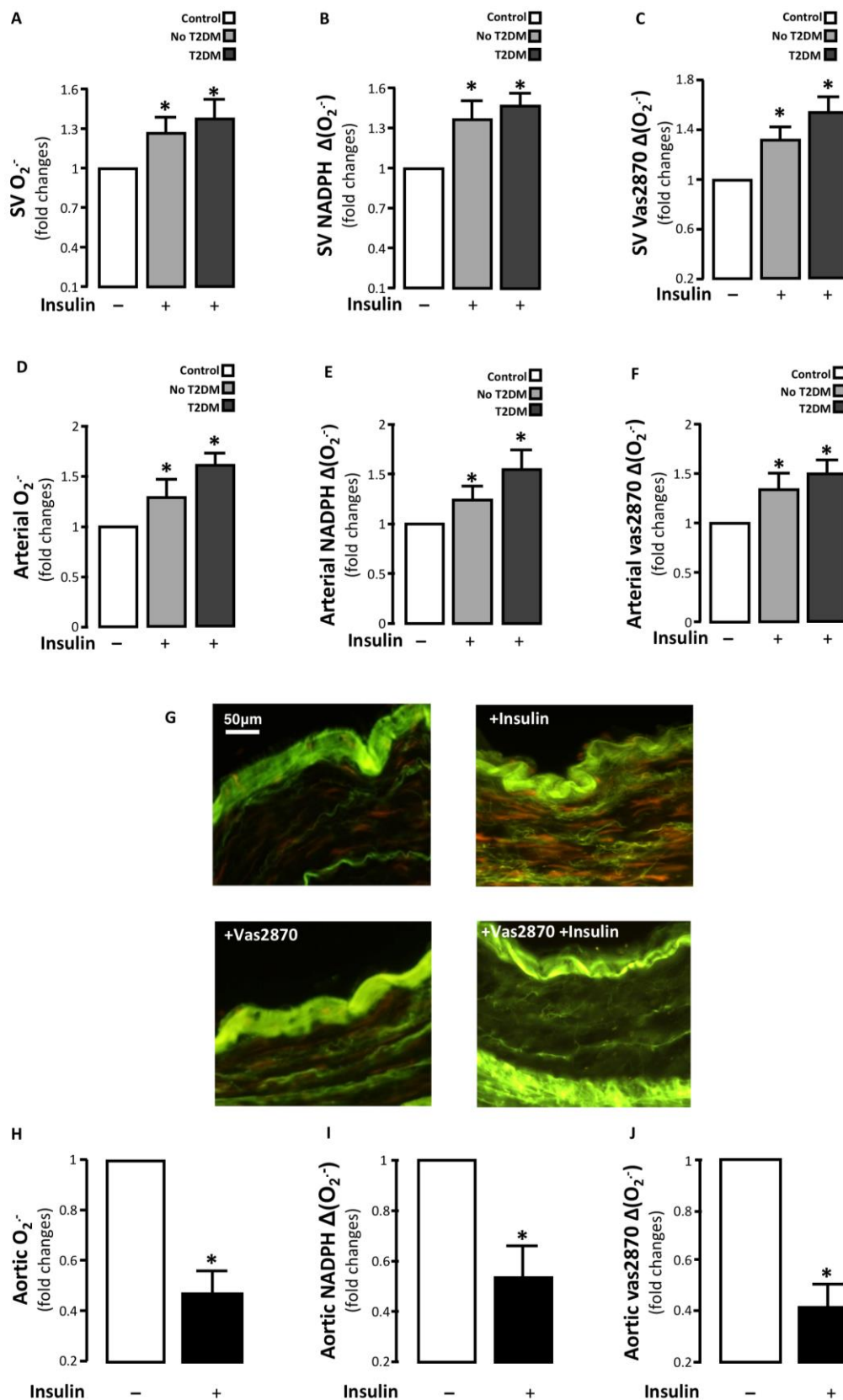


**Fig. 2. Insulin increases NADPH-oxidases activity in vessels from patients with coronary atherosclerosis.** (A-C) Effect of exogenous insulin (glargine M1, 10 nM) on basal (A, n = 7

pairs), NADPH-stimulated (B, n = 7 pairs), and Vas2870-inhibitable (C, n = 7 pairs) superoxide ( $O_2^{\cdot-}$ ) in saphenous vein (SV) segments. (D-F) Effect of exogenous insulin (glargine M1, 10 nM) on basal (D, n = 5 pairs), NADPH-stimulated (E, n = 5 pairs), and Vas2870-inhibitable (F, n = 5 pairs)  $O_2^{\cdot-}$  in internal mammary artery (IMA) segments. HOMA-IR for patients without diabetes was 1.64[0.87-2.73] (median[25<sup>th</sup>-75<sup>th</sup> percentile]. (G) Example dihydroethidium (DHE) staining images for in situ visualization of basal and Vas2870-inhibitable  $O_2^{\cdot-}$  production in response to insulin (glargine M1, 10 nM) in IMA. DHE staining appears as red and auto-fluorescence as green (H-J) Effects of ex vivo insulin incubation (glargine, 10 nM) on basal (H, n = 5 pairs), NADPH-stimulated (I, n = 5 pairs) and Vas2870-inhibitable (J, n = 5 pairs)  $O_2^{\cdot-}$  generation in aortic tissue from wild type mice. \* $P < 0.05$  vs control after Bonferroni correction in panels A-F.  $P = 0.048$  vs control for panels H-J by Wilcoxon sign rank tests. Patients with diabetes receiving an oral dipeptidyl peptidase 4 (DPP4) inhibitor were excluded from these experiments.  $P$ -values are calculated by Wilcoxon sign rank test in panels A-F, H-J; data are presented as mean  $\pm$  SEM.

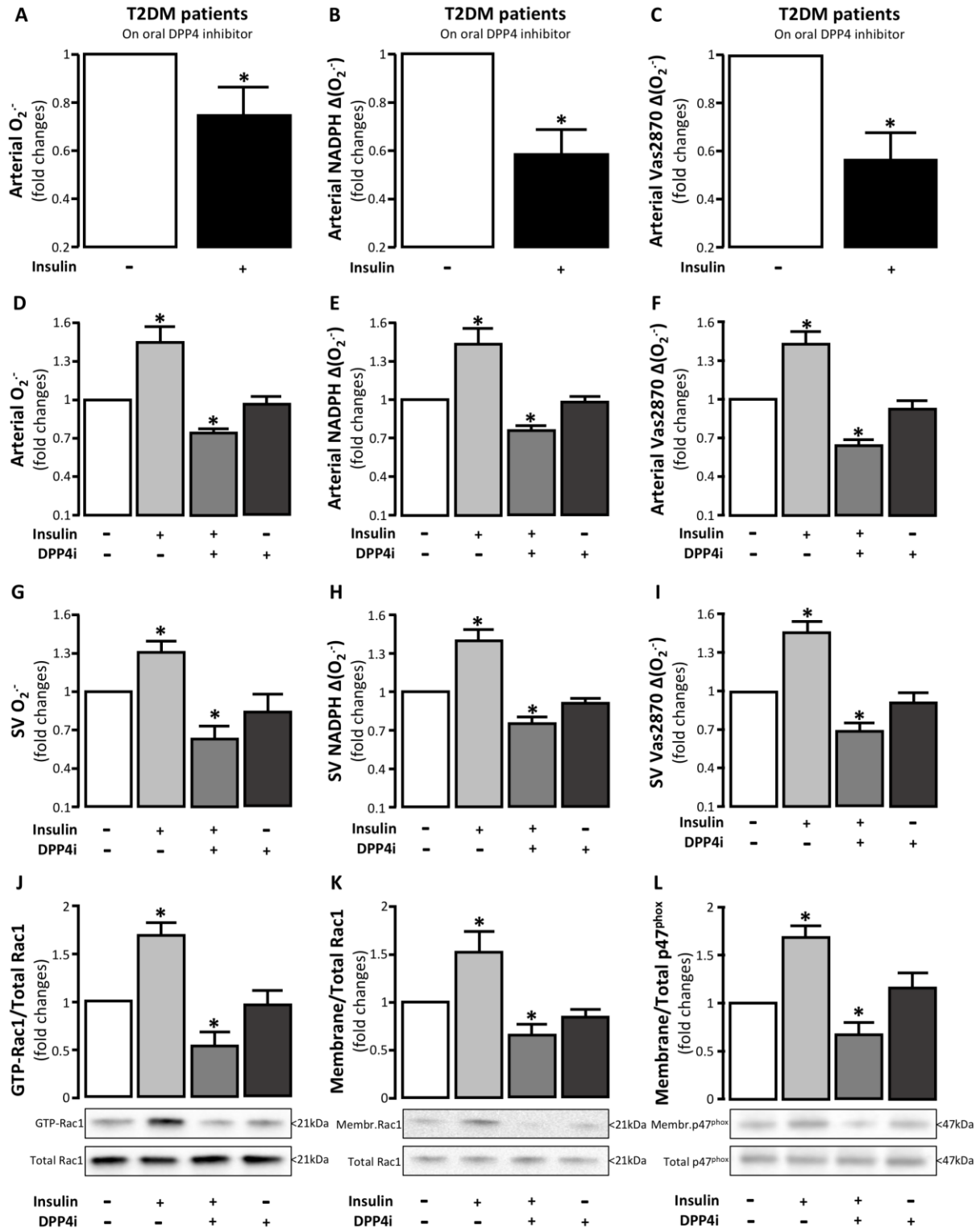


**Fig. 3. DPP4 inhibition modulates the activation of vascular NADPH-oxidases in response to insulin in humans.** (A-C) Effect of ex vivo insulin incubation (glargine M1, 10 nM) on basal (A, n = 5 pairs), NADPH-stimulated (B, n = 5 pairs), and Vas2870-inhibitable (C, n = 5

pairs) superoxide ( $O_2^{\cdot-}$ ) in saphenous vein (SV) segments of a subgroup of patients with diabetes receiving oral DPP4 inhibitor (DPP4i) treatment in vivo. **(D-F)** Effect of ex vivo insulin incubation (glargine M1, 10 nM) on basal (D, n = 10), NADPH-stimulated (E, n = 10), and Vas2870-inhibitable (F, n = 10,)  $O_2^{\cdot-}$  in internal mammary artery (IMA) with or without ex vivo preincubation with DPP4-i KR62436 (70  $\mu$ M). **(G-I)** Effect of ex vivo insulin incubation (glargine M1, 10 nM) on basal (G, n = 13), NADPH-stimulated (H, n = 13), and Vas2870-inhibitable (I, n = 13)  $O_2^{\cdot-}$  in SV with or without ex vivo DPP4i preincubation. **(J-L)** Effect of ex vivo insulin incubation (glargine M1, 10 nM) on (J) Rac1 GTP-activation (n = 5), (K) membrane translocation of active Rac1 (n = 5), and (L) the p47<sup>phox</sup> subunit (n = 5)  $O_2^{\cdot-}$  in human SV with or without ex vivo DPP4-I preincubation).  $P = 0.047$  by Wilcoxon sign-rank test in panels A-C.  $*P < 0.05$  vs control by Wilcoxon sign rank test in panels D-L followed by Bonferroni correction as appropriate; data presented as mean  $\pm$  SEM.

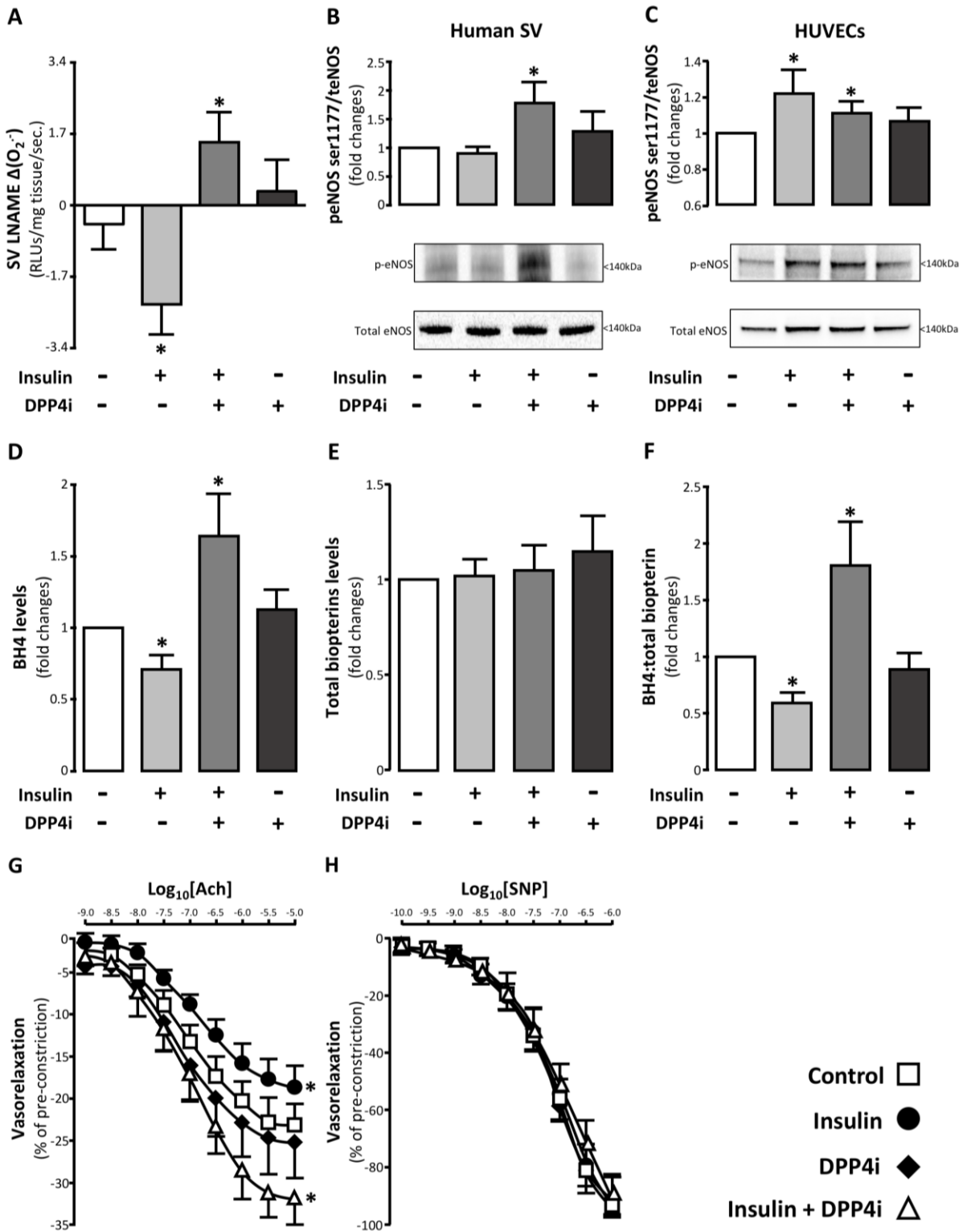


**Fig. 4. DPP4 regulates the effect of insulin on vascular endothelial nitric oxide synthase (eNOS) coupling in humans.** (A) Effect of ex vivo insulin incubation (glargine M1, 10 nM) on eNOS uncoupling evidenced by the LNAME-induced reduction of vascular superoxide

(LNAME- $\Delta(\text{O}_2^-)$ ) in the presence or absence of DPP4 inhibitor (DPP4i) pre-incubation (A, n=5-7 per intervention). **(B-C)** Effect of insulin (glargine M1, 10 nM) on the phosphorylation of eNOS at ser1177 in (B) human saphenous vein (SV) segments (n = 5) versus (C) human umbilical vein endothelial cells (HUVEC) in vitro (n =5) in the presence or absence of DPP4i preincubation. **(D-F)** Effect of ex vivo insulin (glargine M1, 10 nM on (D) vascular tetrahydrobiopterin (BH4) content (n = 5), (E) total biopterin content (n = 5), and (F) BH4 bioavailability ( n = 5) in the presence or absence of DPP4i. **(G-H)** Effect of ex vivo insulin (glargine M1, 10 nM)/DPP4i incubations on (G) endothelium-dependent acetylcholine (Ach) vasorelaxations (n = 5 – 6 per intervention) and (H) endothelium-independent sodium nitroprusside (SNP) vasorelaxations (n= 5 – 6 per intervention). \* $P < 0.05$  vs control.  $P$ -values are calculated by Wilcoxon sign rank tests in panels A-F and by two-way ANOVA for matched observations in panels G-H. Data presented as mean  $\pm$  SEM.

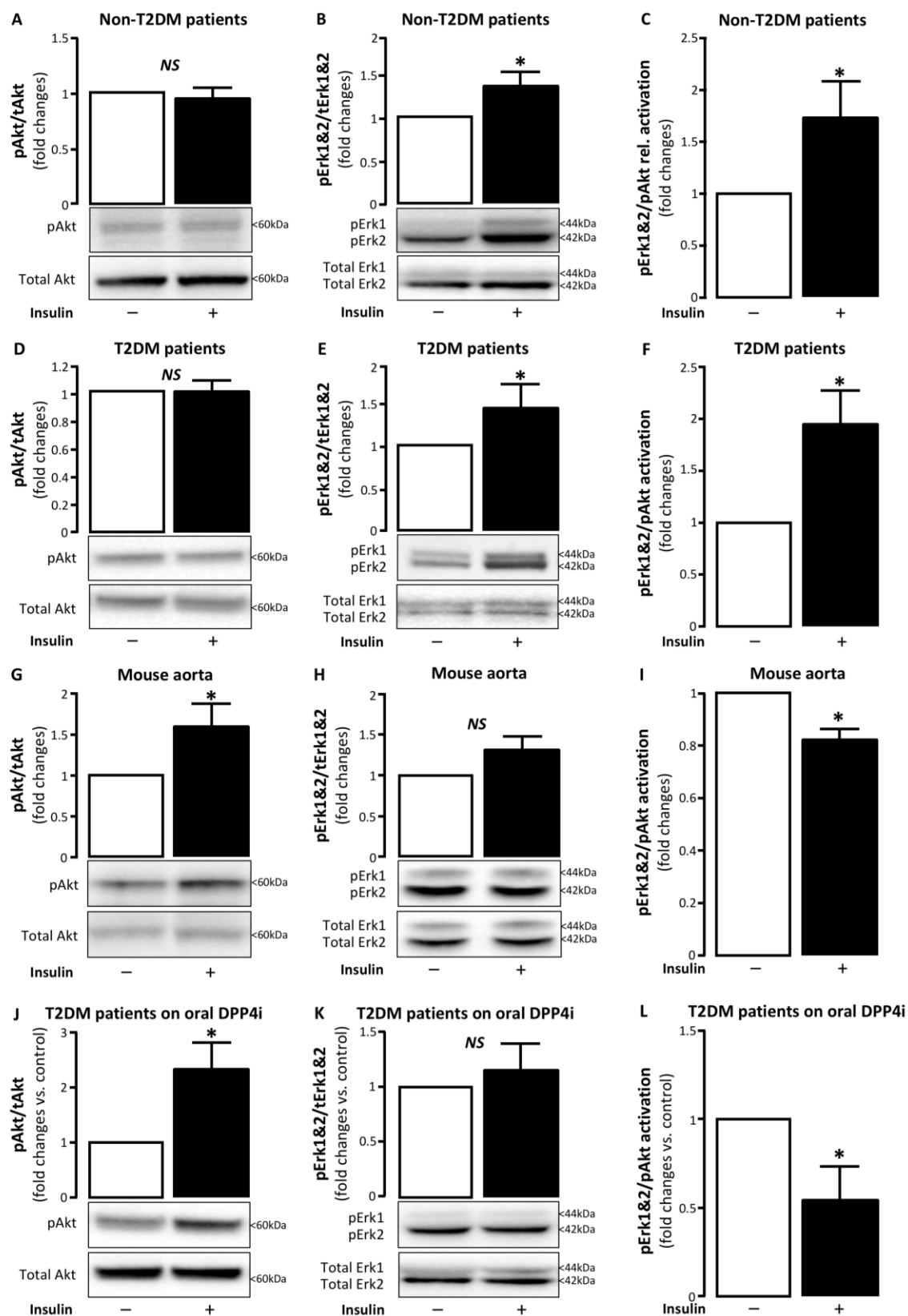


**Fig. 5. The human vascular wall is characterized by vascular insulin resistance (IR), and this is reversed by dipeptidyl peptidase 4 inhibition. (A-C) Effect of ex vivo insulin**

(glargine M1, 10 nM) on the phosphorylation of (A) Akt (n = 5), (B) Erk1&2 (n = 5), and (C) the balance of the two (n = 5) in the human vascular wall (saphenous veins, SV) in patients without diabetes and with coronary atherosclerosis. **(D-F)** Effect of ex vivo insulin (glargine M1, 10 nM) on the phosphorylation of (D) Akt (n = 5), (E) Erk1&2 (n = 5), and (F) the balance of the two (n = 5) in SV of patients with diabetes and coronary atherosclerosis. **(G-I)** Effect of ex vivo insulin (glargine M1, 10 nM) on the phosphorylation of (G) Akt (n = 5), (H) Erk1&2 (n = 5), and (I) the balance of the two (n = 5) in atherosclerosis-free wild-type mouse aortic tissue. **(J-L)** effect of ex vivo insulin (glargine M1, 10 nM) on the phosphorylation of (J) Akt (n = 5), (K) Erk1&2 (n = 5), and (L) the balance of the two (n = 5) in the human vascular wall (saphenous veins, SV) in patients with diabetes on oral DPP4 inhibitor (DPP4i) treatment. \* $P < 0.05$ ; NS Non significant vs control.  $P$ -values are calculated by Wilcoxon sign rank tests in all panels. Data presented as mean  $\pm$  SEM.

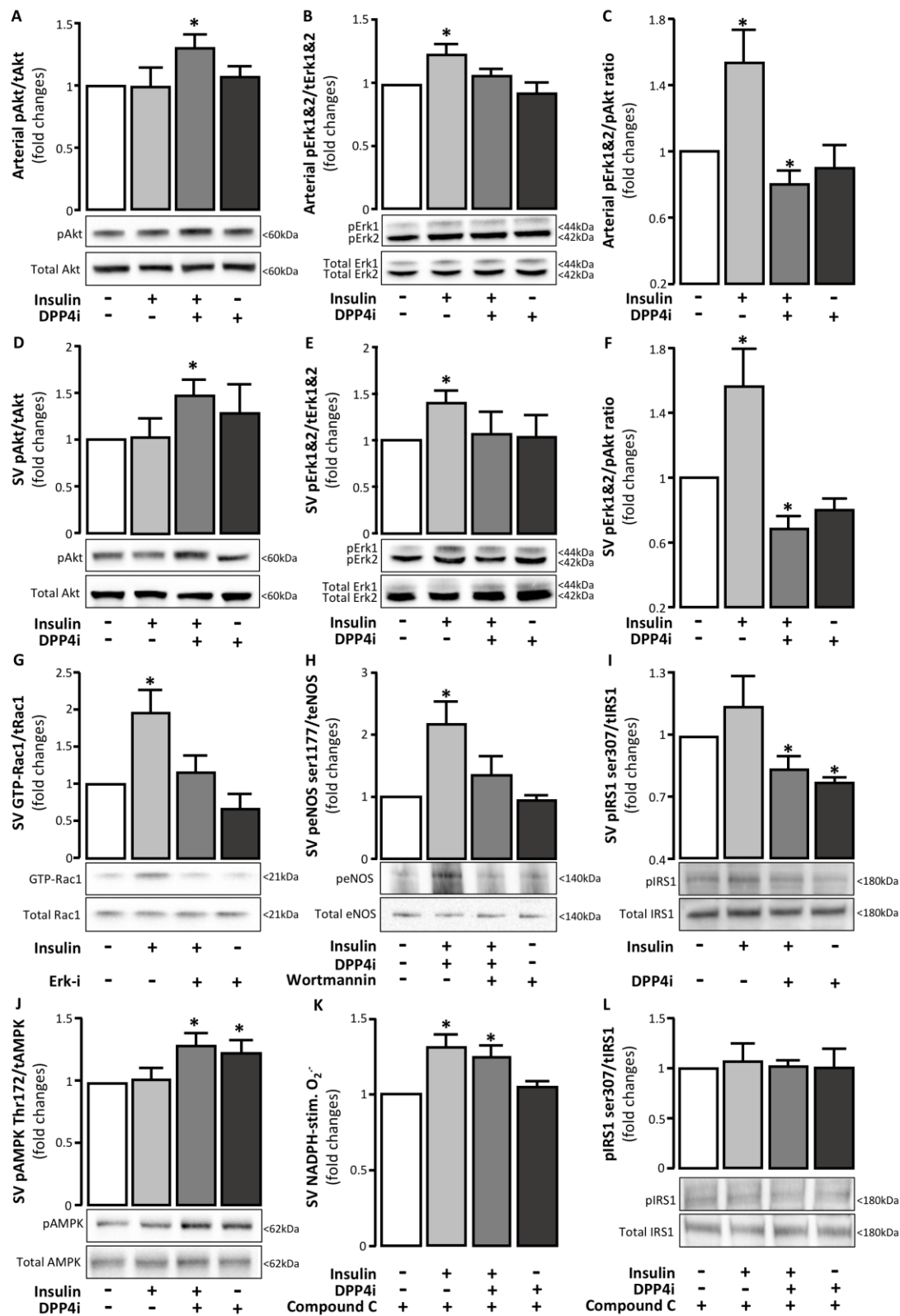


**Fig. 6. Dipeptidyl peptidase 4 inhibition regulates vascular insulin signalling via restoring local insulin sensitivity in an AMPK-dependent manner. (A-C)**

Effect of DPP4i on insulin (glargine M1, 10 nM)-stimulated phosphorylation of (A) Akt (n =

5), (B) Erk1&2 (n = 5), and (C) the balance between the two (n = 5) in human internal mammary artery (IMA) segments. **(D-F)** Effect of DPP4i on insulin (glargine M1, 10 nM)-stimulated phosphorylation of (D) Akt (n = 5-7), (E) Erk1&2 (n = 5-7), and (F) the balance between the two (defined as the ratio of pAkt/pErk1&2, n = 5-7) in human saphenous vein (SV) segments. **(G)** Effect of Erk1&2 inhibition using 3-(2-Aminoethyl)-5-((4-ethoxyphenyl)methylene)-2,4-thiazolidinedione (70  $\mu$ M) on insulin (glargine, 10nM)-stimulated Rac1 activation (n = 5-6). **(H)** Effect of Akt inhibition using wortmannin (100 nM) on the ability of insulin (glargine M1, 10 nM)/DPP4i combination to induce endothelial nitric oxide synthase (eNOS) ser1177 phosphorylation (n = 5-8). **(I)** Effect of DPP4i on insulin response substrate 1 (IRS1) Ser307 phosphorylation, a site linked with molecular IR (n = 5 pairs). **(J)** Effect of DPP4i on AMPK Thr172 phosphorylation (n = 5-7). **(K)** Consequence of AMPK pre-inhibition on the effects of insulin (glargine M1, 10 nM)/DPP4i incubations on vascular NADPH-stimulated  $O_2^-$  (n = 5). **(L)** Consequence of AMPK pre-inhibition by compound C on the effect of DPP4i on vascular IRS1 Ser307 phosphorylation (n = 5). \* $P < 0.05$  vs control.  $P$ -values are calculated by Wilcoxon sign rank tests in all panels. Data presented as mean  $\pm$  SEM.

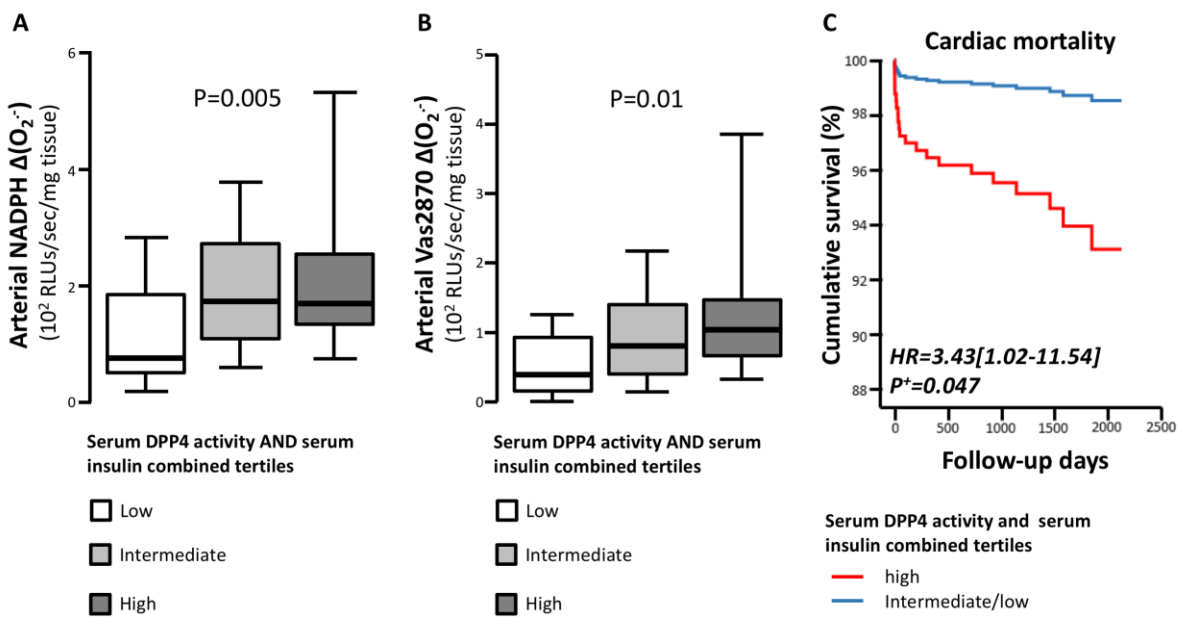


**Fig. 7. Clinical implications of the interactions between systemic DPP4 activity and insulin.** (A-B) Associations of arterial NADPH-stimulated (A) and Vas2870-inhibitable (B)  $O_2^{\cdot-}$  with combined serum insulin and DPP4 activity tertiles in study 1 (n=580). (C) Association of combined high serum insulin and serum DPP4 activity with relative risk for cardiac death after adjustment for other risk factors (EuroSCORE II, hyperlipidaemia, hypertension, NYHA class and circulating hsCRP). *P*-values in panels A-B are calculated by Kruskal Wallis tests. In panel C, the hazard ratio and *P*<sup>+</sup> value presented are calculated from Cox regression after adjusting for EuroSCORE II, hyperlipidaemia, hypertension, NYHA class and circulating hsCRP. Hazard ratio is presented as HR[95% confidence intervals]. Data presented as median[25<sup>th</sup>-75<sup>th</sup> percentile] in panels A-B.

## Tables

**Table 1. Demographic characteristics of study participants.**

|                                      | Study 1         | Study 2         | P-value |
|--------------------------------------|-----------------|-----------------|---------|
| Participants (n)                     | 580             | 94              |         |
| Age (years)                          | 66.8±0.4        | 68.3±1.0        | 0.167   |
| Males (%)                            | 81.1            | 88.6            | 0.100   |
| Hypertension (%)                     | 72.1            | 78.2            | 0.300   |
| Hyperlipidaemia (%)                  | 77.7            | 93.2            | <0.001  |
| Type 2 diabetes mellitus (%)         | 21.7            | 31.8            | 0.042   |
| Smoking                              |                 |                 | 0.344   |
| Active (%)                           | 10.1            | 6.9             |         |
| Past (%)                             | 54.0            | 49.4            |         |
| BMI (kg/m <sup>2</sup> )             | 28.5±0.2        | 28.5±0.4        | 0.928   |
| Waist-to-hip ratio                   | 0.98±0.01       | 0.99±0.01       | 0.715   |
| HOMA-IR in patients without diabetes | 1.16[0.73-1.83] | 1.26[0.53-1.82] | 0.534   |
| Plasma hsCRP (mg/L)                  | 1.40[0.60-4.10] | 1.20[0.50-2.35] | 0.549   |
| <b>Medication</b>                    |                 |                 |         |
| Antiplatelet (%)                     | 81.2            | 83.5            | 0.678   |
| ACEi/ARBs (%)                        | 61.9            | 68.3            | 0.456   |
| Statins (%)                          | 82.0            | 88.0            | 0.214   |
| β-blockers (%)                       | 65.9            | 74.7            | 0.127   |
| Calcium channel blockers (%)         | 25.6            | 31.3            | 0.287   |
| Insulin (%)                          | 7.4             | 8.4             | 0.662   |
| Oral hypoglycemics (%)               | 15.5            | 25.3            | 0.023   |

BMI: Body mass index; HOMA-IR: Homeostatic model assessment – insulin resistance; hsCRP: High sensitivity C-reactive protein; ACEi: Angiotensin converting enzyme inhibitor; ARB: Angiotensin receptor blocker; Age and BMI are presented as mean ± standard error of the mean; HOMA-IR is presented as median[25<sup>th</sup>-75<sup>th</sup> percentile]; P-values are calculated by Fischer's exact tests for categorical variables, by unpaired t-tests for continuous normally distributed variables (age, BMI and Waist-to-hip ratio) and by Mann Whitney U tests for continuous non-normally distributed variables (HOMA-IR, hsCRP).

**Table 2. Multivariate Cox regression model for survival in study 1.**

|                          | Predictors                    | HR[95% CI], P <sup>+</sup> |
|--------------------------|-------------------------------|----------------------------|
| <b>Cardiac mortality</b> | High serum DPP4/High insulin* | 3.30[1.01-10.77], P=0.048  |
|                          | EuroSCORE II (per SD)*        | 1.70[1.44-2.00], P<0.001   |
|                          | Smoking                       | 1.99[0.24-16.66], P=0.526  |
|                          | Hypertension                  | 0.93[0.29-2.93], P=0.894   |
|                          | Hyperlipidaemia               | 1.16[0.43-3.12], P=0.769   |
|                          | hsCRP (per SD)                | 1.03[0.99-1.06], P=0.158   |

DPP4: Dipeptidyl peptidase 4; hsCRP: high sensitivity C-reactive protein; HR: Hazard ratio; \* denotes the independently significant predictors; +adjusted value

## **Dipeptidyl peptidase 4 inhibition ameliorates insulin-induced vascular redox dysregulation in human atherosclerosis**

Ioannis Akoumianakis<sup>1</sup>, Ileana Badi<sup>1</sup>, Gillian Douglas<sup>1</sup>, Surawee Chuaiphichai<sup>1</sup>, Laura Herdman<sup>1</sup>, Nadia Akawi<sup>1</sup>, Marios Margaritis<sup>1</sup>, Alexios S. Antonopoulos<sup>1</sup>, Evangelos K. Oikonomou<sup>1</sup>, Costas Psarros<sup>1</sup>, Nikolaos Galiatsatos<sup>2</sup>, Dimitris Tousoulis<sup>3</sup>, Attila Kardos<sup>4</sup>, Rana Sayeed<sup>5</sup>, George Krasopoulos<sup>5</sup>, Mario Petrou<sup>5</sup>, Uwe Schwahn<sup>6</sup>, Paulus Wohlfart<sup>6</sup>, Norbert Tennagels<sup>6</sup>, Keith M. Channon<sup>1</sup>, Charalambos Antoniades<sup>1</sup>

### **Affiliations:**

<sup>1</sup> Division of Cardiovascular Medicine, Radcliffe Department of Medicine, University of Oxford, UK, OX3 9DU

<sup>2</sup> Biochemistry Department, Hippokration General Hospital, Athens, Greece, 115 27

<sup>3</sup> First Cardiology Clinic, Athens University Medical School, Greece, 115 27

<sup>4</sup> Milton Keynes University Hospital NHS Foundation Trust & Faculty of Life Sciences University of Buckingham, UK, MK6 5LD

<sup>5</sup> Cardiothoracic Surgery Department, Oxford University Hospitals NHS Foundation Trust, UK, OX3 9DU

<sup>6</sup> Sanofi Aventis Deutschland GmbH, Germany, D-65926

**Single-sentence summary:** Insulin causes vascular oxidant stress in human atherosclerosis that is reversed by dipeptidyl-peptidase-4 inhibition by restoring insulin sensitivity

### **Corresponding author:**

Charalambos Antoniades MD PhD FESC  
Professor of Cardiovascular Medicine University of Oxford  
John Radcliffe Hospital, Oxford OX3 9DU  
United Kingdom  
e-mail: antoniad@well.ox.ac.uk  
Tel: +441865228340

## Supplementary Material

### Supplementary Methods

#### *Blood sampling and circulating biomarker measurements*

Venous blood was collected prior to surgery after 8h of fasting, serum or plasma was isolated by centrifugation at 3,000g for 15min at 4°C and stored at -80°C until assayed. Serum glucose was measured by the hexokinase method using commercially available kits (Abbott). Serum insulin was measured by a chemiluminescent microparticle immunoassay using commercially available kits (Abbott). Plasma hsCRP was measured by the high-sensitivity latex enhanced immunoturbidimetric assay (ADVIA, Bayer HealthCare LLC). Serum IL6 and TNF $\alpha$  were measured by the Quantikine HS ELISA Human IL-6 Immunoassay (order ID: HS600C) and Quantikine HS ELISA Human TNF $\alpha$  Immunoassay (order ID: HSTA00E) from R&D Systems according to the manufacturer's instructions.

Homeostatic model assessment of systemic IR (HOMA-IR) was calculated by using the formula  $(\text{glucose} \times \text{insulin})/405$ , with glucose measured in mg/dL and insulin in mU/L. HOMA-IR is an established and frequently used surrogate marker of IR, mainly hepatic IR (44) as opposed to tissue-specific variations in peripheral IR (45). HOMA-IR is also a less sensitive marker of genetic susceptibility to IR (46) and IR presence in normal or near normal weight patients (presumably because of the interference of adiposity & obesity with the insulin-glucose feedback) (47). For epidemiological purposes, HOMA-IR correlates well with clinical markers of cardiometabolic disease and it is useful in concisely reflecting the overall variations in whole body IR (44, 46).

### ***Vessel harvesting***

Internal mammary artery (IMA) and saphenous vein (SV) samples were harvested with a “no touch” technique at the time of CABG. Vascular segments were transferred into oxygenated (95% O<sub>2</sub> / 5% CO<sub>2</sub>) ice-cold Krebs Hensleit buffer and the vessel lumen was flushed gently by using an insulin syringe to remove blood. Each vessel was separated from its adipose tissue in the lab, under magnification by the same operator, to limit the between-patients variability. The same anaesthetics were used in all cases, and each sample was always obtained at the same stage of the operation, to limit the between-patients variability.

### ***Ex vivo human tissue incubations***

Serial vascular segments obtained from individual patients were incubated for 20min at 37°C, 95% O<sub>2</sub> in the presence or absence of insulin. Human insulin and two synthetic insulin analogues (the active metabolite M1 of insulin glargine or degludec) were used for these incubations (all supplied by Sanofi Aventis GmbH). All insulins were used at 1nM, 10nM and 100nM for screening dose-response experiments as well as at fixed concentrations for further *ex vivo* mechanistic experiments (10nM for human insulin and M1 glargine, 100nM for Degludec as per our dose-response experiment results and published pharmacodynamics of these insulin types). To evaluate the effects of DPP4i, serial vascular segments from some patients were pre-incubated with KR62436 70µM, a chemical inhibitor of DPP4 (Sigma), 37°C, 95% O<sub>2</sub> starting 15min prior to the 20min insulin incubations. In certain sub-groups of patients, vascular segments were pre-incubated with compound C (an inhibitor of AMPK) 10µM for 20 min, exendin 3 (9-39 amide, a GLP1R antagonist) 100nM for 30 min or enzastaurin (a PKCβ inhibitor) 30nM for 20 min before the aforementioned experimental conditions, in order to

evaluate the role of AMPK, GLP1R and PKC $\beta$  in the crosstalk between DPP4i and insulin signalling.

### ***Vasomotor studies***

Human vasomotor studies were performed in SV segments obtained during CABG as we have previously described (18, 41). Vessels were equilibrated in the organ bath for 60 minutes, in oxygenated (95% O<sub>2</sub>/5% CO<sub>2</sub>) Krebs-Hensleit buffer at 37°C to achieve a resting tension of 3g. Contractile responses were tested by exposure to Krebs-Hensleit buffer containing potassium chloride (60mM). Four rings from each vessel were pre-contracted with phenylephrine (3x10<sup>-6</sup>M); then endothelium-dependent relaxations were quantified using acetylcholine (ACh, 10<sup>-9</sup>M to 10<sup>-5.5</sup>M) and/or bradykinin (BK, 10<sup>-9</sup>M to 10<sup>-5.5</sup>M). Finally, relaxations to the endothelium-independent NO donor sodium nitroprusside (SNP, 10<sup>-10</sup>M to 10<sup>-6</sup>M), were evaluated in the presence of the NOS inhibitor NG-nitro-L-arginine methyl ester (L-NAME; 100 $\mu$ M), as we have previously described (18, 41, 42).

Mouse vasomotor function was analysed using isometric tension studies in a wire myograph (Multi-Myograph 610M, Danish Myo Technology, Denmark). Briefly, rings isolated from the thoracic aorta were mounted on a wire myograph containing 5ml of Krebs-Henseleit buffer (in [mmol/l]: NaCl 120, KCL 4.7, MgSO<sub>4</sub> 1.2, KH<sub>2</sub>PO<sub>4</sub> 1.2, CaCl<sub>2</sub> 2.5, NaHCO<sub>3</sub> 25, glucose 5.5) at 37°C, gassed with 95% O<sub>2</sub>/5% CO<sub>2</sub>. After a 30min equilibration period, optimal tension was set, ring viability was tested with 60 mM KCL and endothelium-dependent dose-response curves in response to acetylcholine were recorded following 20min insulin (glargine, 10nM) or control incubations and phenylephrine pre-constriction. Endothelium-independent vasorelaxations in response to SNP were finally evaluated in the presence of L-NAME. Results are expressed as % of phenylephrine pre-constriction.

***Vascular superoxide measurements***

Vascular  $O_2^{\cdot -}$  production was measured in fresh, intact IMA and SV segments as well as mouse aortic tissue by using lucigenin (5  $\mu\text{mol/L}$ )-enhanced chemiluminescence, as we have described previously (18). Vessels were opened longitudinally to expose the endothelial surface and equilibrated for 20 minutes in oxygenated (95%  $O_2$ /5%  $CO_2$ ) Krebs-HEPES buffer (pH 7.4) at 37°C. The contribution of uncoupled nitric oxide synthase (NOS) to vascular  $O_2^{\cdot -}$  production was quantified as the change of  $O_2^{\cdot -}$  from baseline to 20 minutes after incubation with the NOS inhibitor L-NAME (100  $\mu\text{mol/L}$ ), and presented as delta-LNAME  $O_2^{\cdot -}$  as we have previously described (18, 41, 42).

***Xanthine/xanthine oxidase  $O_2^{\cdot -}$ -scavenging experiments***

The scavenging properties of DPP4i were evaluated by lucigenin (5 $\mu\text{M}$ ) chemiluminescence using the xanthine (0.5 mM)/xanthine oxidase (0.02 U/ml) chemical enzymatic system to generate  $O_2^{\cdot -}$  as previously described (47). Overall  $O_2^{\cdot -}$  was recorded in the presence or absence of DPP4i. Results are expressed in  $10^5\text{xRLU/sec}$ .

***Vascular biopterin measurements***

Vascular BH<sub>4</sub>, dihydrobiopterin (BH<sub>2</sub>), and biopterin (B) were each determined separately from the same sample, using high-performance liquid chromatography followed by serial electrochemical and fluorescent detection, as we have previously described (18). Total biopterin is the sum of BH<sub>4</sub>, BH<sub>2</sub>, and B individual concentrations. Biopterin was expressed as pmol/mg of vascular tissue.

***Oxidative fluorescent microscopy***

In situ  $O_2^-$  production was determined in vessel cryosections with oxidative fluorescent dye dihydroethidium (DHE), as previously described (42). IMA rings were snap frozen in OCT. Cryosections (30  $\mu$ m) were incubated with DHE (2  $\mu$ mol/L for 5 minutes) in Kreps-Hepes buffer, with or without Vas2870 (400  $\mu$ mol/L). Fluorescence images of the endothelium (x63, Zeiss LSM 510 META laser scanning confocal microscope) were obtained from each vessel quadrant. In each case, segments of vessel rings ( $\pm$  Vas2870) were analysed in parallel with identical imaging parameters in a blinded fashion.

***Vascular Rac1 activation assay***

Rac1 activation was evaluated by a commercially available affinity precipitation assay (Cell Signalling Technology, #8815). Briefly, vascular segments were homogenised in ice-cold lysis/binding/wash buffer (Cell Signalling Technology, Cat # 11524) supplemented with 1mM Phenylmethanesulfonyl fluoride (PMSF) (Cell Signalling Technology, #8553). Total protein of tissue homogenates was quantified by the Pierce BCA protein assay kit (ThermoFischer Scientific, #23225). Affinity precipitation of Rac1 was performed using agarose beads and GST-PAK1-PBD added in 500 mg of protein homogenates in spin caps, followed by 1h incubation at 4°C. Samples were subsequently washed three times and active GTPases were separated from agarose beads by elution in reducing loading buffer. Eluted samples were heated at 95°C for 5 min and then stored in -80°C until used for Western immunoblotting.

***Vascular p47<sup>phox</sup> and Rac1 membrane translocation***

Membrane translocation of Rac1 and p47<sup>phox</sup> was estimated by differential centrifugation of vascular homogenates to isolate membrane proteins, and membrane-translocated Rac1 or p47<sup>phox</sup> protein was determined by Western immunoblotting as previously described (40). Briefly, vascular segments were homogenized in ice-cold HEPES buffer (20 HEPES mM, 150mM NaCl, and 1mM EDTA, pH 7.4) supplemented with a protease inhibitor cocktail (Roche, UK). Debris was removed by centrifugation of the homogenates at 2,800 g at 4°C for 20min, and protein content of supernatants was evaluated by the Pierce BCA protein assay kit. 500mg of total protein were adjusted to 200μL for all samples, added into ultracentrifugation tubes and ultra-centrifuged at 100,000 g for 60 min at 4°C to separate cytosolic from membrane proteins. Following removal of supernatants containing the cytosolic proteins, pellets were re-suspended in 35 μL of lysis buffer containing 1% Triton and left for 20 min on ice. Protein concentrations were quantified and the samples were processed for Western immunoblotting as described below.

***Immunoprecipitation of IRS1***

Human vascular segments were first homogenised in a weight-adjusted volume of radioimmunoprecipitation assay (RIPA) buffer (Cell Signalling Technology, #9806) containing a protease and phosphatase inhibitor cocktail (Cell Signalling Technology, #5871 and #5870 respectively), debris removed by centrifugation at 13,000 rpm for 15 minutes, at 4 °C. Following pre-treatment of the protein lysates with A/G agarose beads (ThermoFischer Scientific, #20423), protein concentrations of samples were quantified by the Pierce BCA protein assay kit. 300-500mg of total protein from all samples were adjusted to an equal volume of 200μL and incubated with primary anti-IRS1 antibody (Cell Signalling Technology, #3407)

overnight at 4°C. Protein A agarose beads (Cell Signalling Technology, #9863) were then added to the samples and incubated for 2h at 4°C. Samples were then washed and immunoprecipitated proteins re-suspended in reducing loading buffer. Samples were heated at 95°C for 5 min and then stored in -80°C until used for Western immunoblotting.

### ***Western blotting***

Western blotting for Akt [Cell Signalling technology, Cat # 4691, 1:2,000, 5% milk in Tris-buffered saline-tween (TBST)]/p-Akt (ser473) [Cell Signalling Technology, Cat # 4060, 1:1,000, 5% bovine serum albumin (BSA) in TBST], eNOS (BD Transduction Labs, Cat # 610296, 1:1,000, 5% BSA in TBST)/p-eNOS (ser1177) (Cell Signalling Technology, Cat # 9570, 1:1,000, 3% BSA in TBST), Erk1&2 (Cell Signalling Technology, Cat # 4695, 1:2,000, 5% milk in TBST)/p-Erk1&2 (Thr202/Tyr204) (Cell Signalling Technology, Cat # 4370, 1:1,000, 5% BSA in TBST), AMPK $\alpha$  (Thr172) (Cell Signalling Technology, Cat # 2532, 1:2,000, 5% milk in TBST)/pAMPK $\alpha$  (Cell Signalling Technology, Cat # 5832, 1:2,000, 5% BSA in TBST), IRS1 (Cell Signalling Technology, Cat # 2390, 1:1,000, 5% milk in TBST)/p-IRS1 (ser307) (Cell Signalling Technology, Cat # 2491, 1:1,000, 5% BSA in TBST), Rac1 (Cell Signalling Technology, Cat # 8631, 1:1,000, 5% BSA in TBST) and p47<sup>phox</sup> (Cell Signalling Technology, Cat # 4301, 1:1,000, 5% milk in TBST) was performed in vessel homogenates as described previously (18, 42). Briefly, vascular tissue samples were homogenized in a weight-adjusted volume of RIPA buffer with protease and phosphatase inhibitors. Homogenates were spun at 13,000 rpm for 15 minutes, at 4 °C. The protein concentration of the supernatants was measured using the Pierce BCA protein assay kit. Protein lysates were separated on 4-12% gradient SDS-NuPAGE protein gels (ThermoFischer Scientific), and proteins transferred to nitrocellulose membranes (Amersham, UK Ltd.), and

blocked with 5% powdered skimmed milk or 5% BSA in TBST for 1h, followed by overnight primary antibody incubation at 4°C. Immunodetection of primary antibodies was performed with horseradish-peroxidase-conjugated secondary antibodies (Sigma) and enhanced chemiluminescence (Amersham Bioscience UK Ltd.) and quantified in relation to the house-keeping protein, GAPDH (Sigma, # G9295)

### ***HUVEC culture experiments for Western blotting***

HUVECs were cultured at 37°C in DMEM medium supplemented with 10% fetal bovine serum and 100 U/mL penicillin, 100 U/mL streptomycin in humidified 5% CO<sub>2</sub> incubator. Insulin incubations were performed with 10nM insulin for 20min in the absence or presence of a DPP4 inhibitor (KR62436, Sigma, at 70µM), and cells were then lysed with RIPA buffer supplemented with protease and phosphatase inhibitors for Western blotting.

### ***Evaluation of NFκB nuclear translocation***

HUVECs at passage 2-3 were seeded at a density of  $1,97 \times 10^4$  cells/cm<sup>2</sup> on coverslips (#631-0153, VWR International Ltd, Lutterworth, United Kingdom) and cultured in complete medium overnight (ON). Cells were then serum-starved ON and the next day they were grown in the absence or presence of 70 µM KR62436 for 15 minutes and stimulated with 20 ng/mL Recombinant Human TNF-alpha Protein (#210-TA-005/CF, R&D Systems, Abingdon, United Kingdom) for 60 minutes to induce NF-κB activation and translocation to the nucleus. HUVECs were then washed twice with PBS, fixed with 4%PFA for 10 minutes at room temperature (RT), washed three times with PBS and permeabilized with PBS-0.05% Triton X-100 for 5 minutes at RT. After three washes with PBS and one hour incubation with 1x Casein Solution (#SP-5020, Vector Laboratories Ltd, Peterborough, United Kingdom) to block

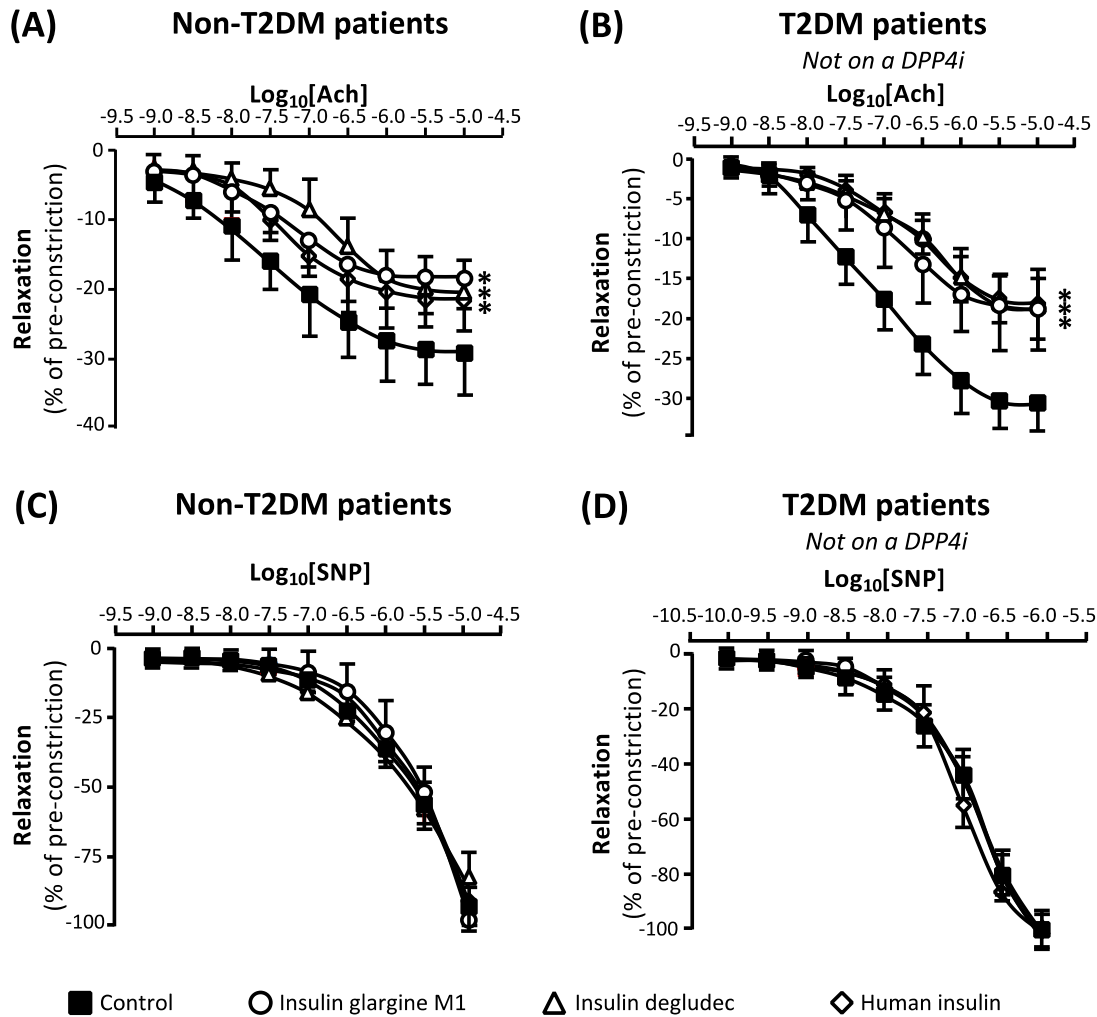
unspecific binding of the antibody, the cells were incubated ON at 4°C with 1 µg/mL anti-NF-κB p65 antibody (#ab16502, Abcam plc, Cambridge, United Kingdom) or with 1 µg/mL Rabbit IgG, polyclonal - Isotype Control (#ab37415, Abcam plc) both diluted in 1x Casein Solution. Samples were then washed three times with PBS and incubated for one hour at RT with 4 µg/mL Goat Anti-Rabbit IgG H&L (Alexa Fluor 488) (#ab150077, Abcam plc) diluted in 1x Casein Solution. After three PBS washes, cells were incubated for one hour at RT with 2 µM TO-PRO™-3 Iodide (TO-PRO-3, #T3605, Thermo Fisher Scientific, Loughborough, United Kingdom) to counter stain the nuclei and then washed three times with PBS. Coverslips were mounted with ProLong Diamond Antifade Mountant with DAPI (#P36962, Thermo Fisher Scientific).

Nuclear:cytoplasmic ratio of NF-κB RelA transcription factor was analysed as previously described (48). Briefly, fluorescence images were captured on a Leica TSC SP5 confocal laser-scanning microscope. To avoid being biased by the NF-κB staining, each field was selected by viewing nuclear (DAPI) staining only to identify near-confluent cells and ten fields were selected for the analysis of each sample. Image analysis was performed using ImageJ 1.52a software (<http://imagej.nih.gov/ij>). For each field, binary image masks (with an automatic thresholding using the Isodata algorithm) of NF-κB and TO-PRO-3 positive staining were created to define the regions of interest (ROI) for the analyses. The TO-PRO-3 staining mask was used to define the nuclear ROI. The cytoplasmic ROI was determined by subtracting the nuclear mask from the NF-κB mask. Each of these ROI masks was utilized to calculate the nuclear:cytoplasmic ratio of NF-κB staining. Five independent experiments were performed and analysed.

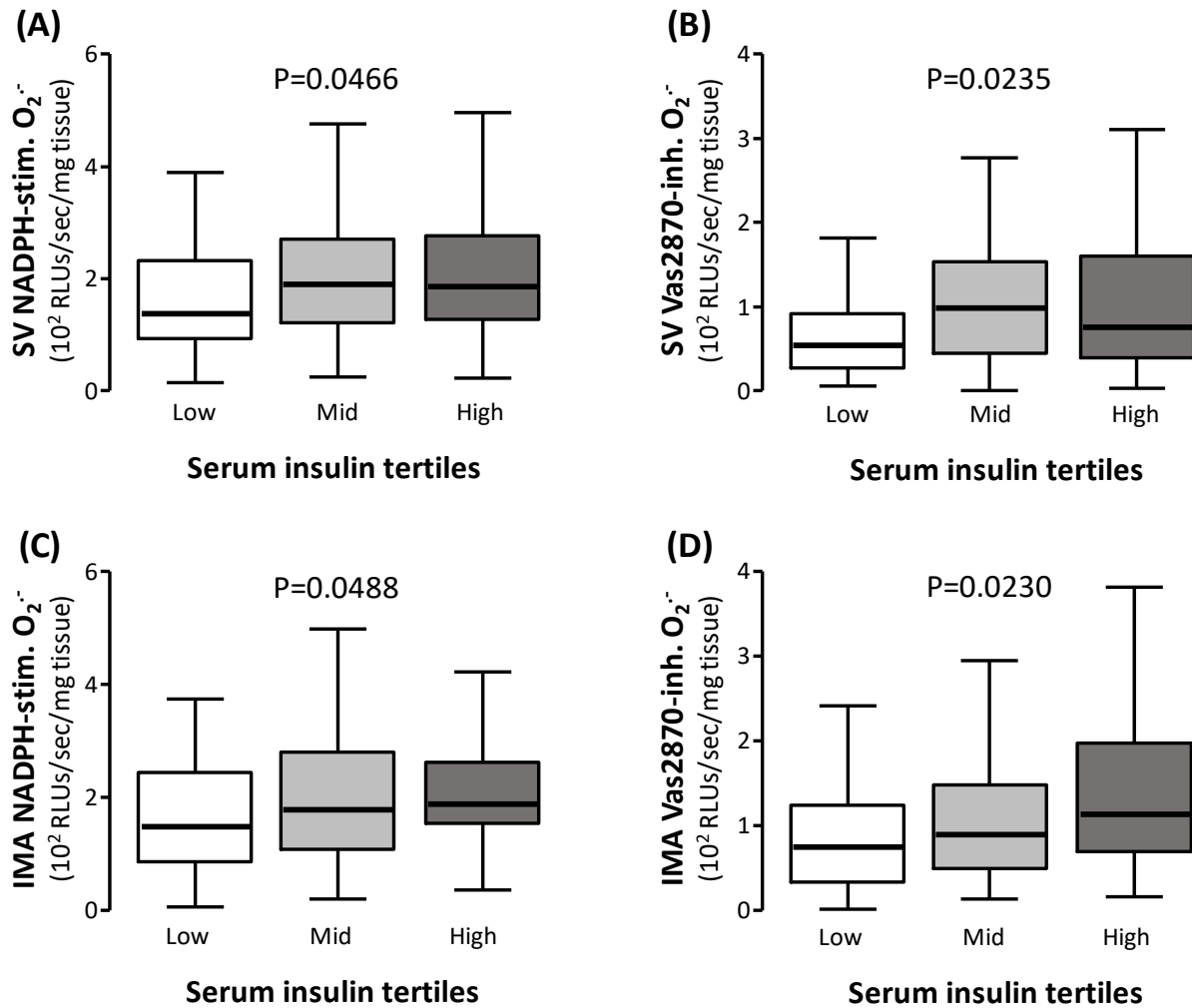
***Sample preparation for transcriptomics profiling***

Serial IMA rings were incubated at 37°C with insulin (glargine, 10nM) for 8h and snap-frozen in -80°C in trizol until further processing. RNA was isolated by the QIAGEN microarray tissue kit as per manufacturer's instructions, and its quality tested with an Agilent bioanalyzer. After passing the quality check, samples were used for high throughput gene expression profiling.

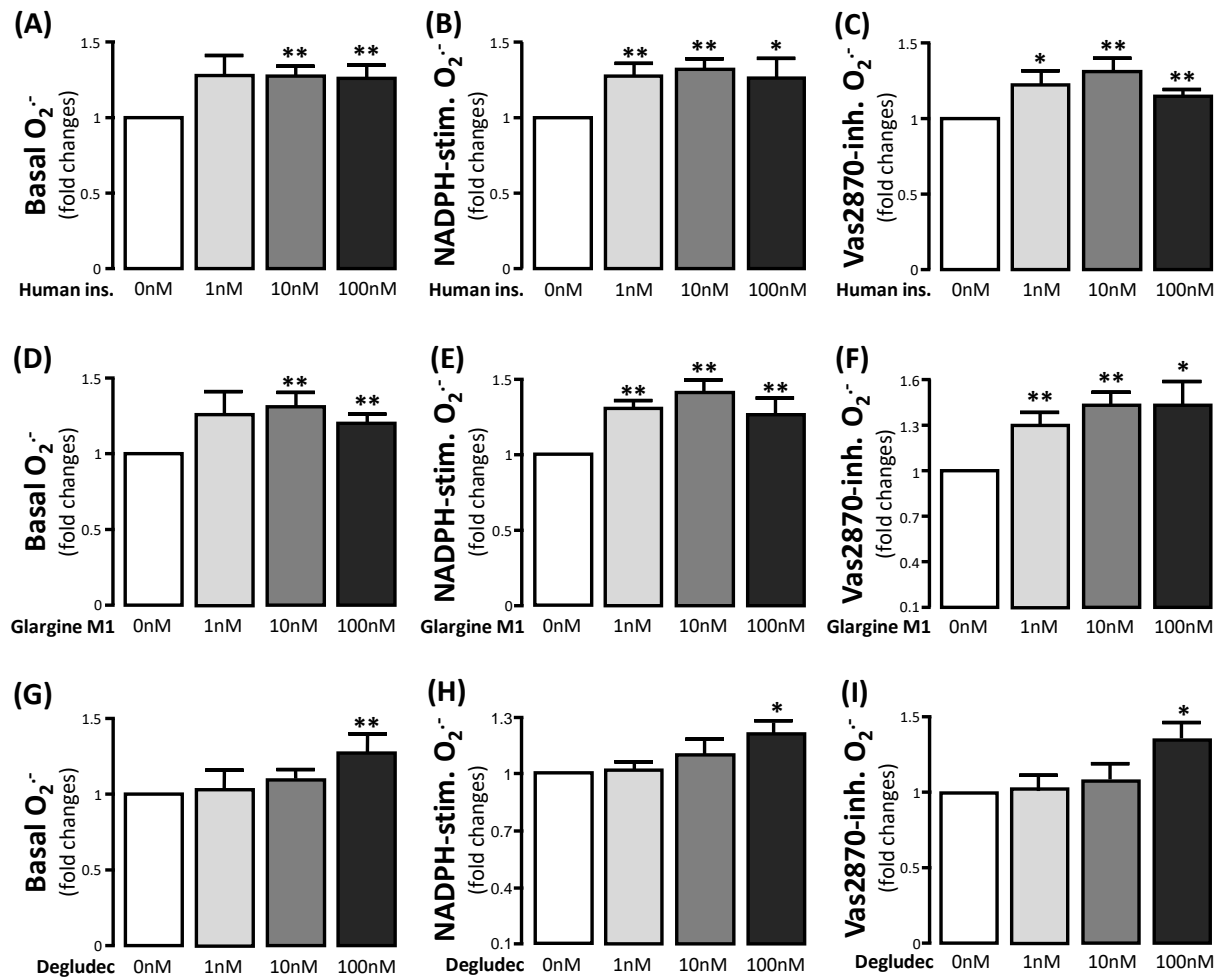
## Supplemental figures



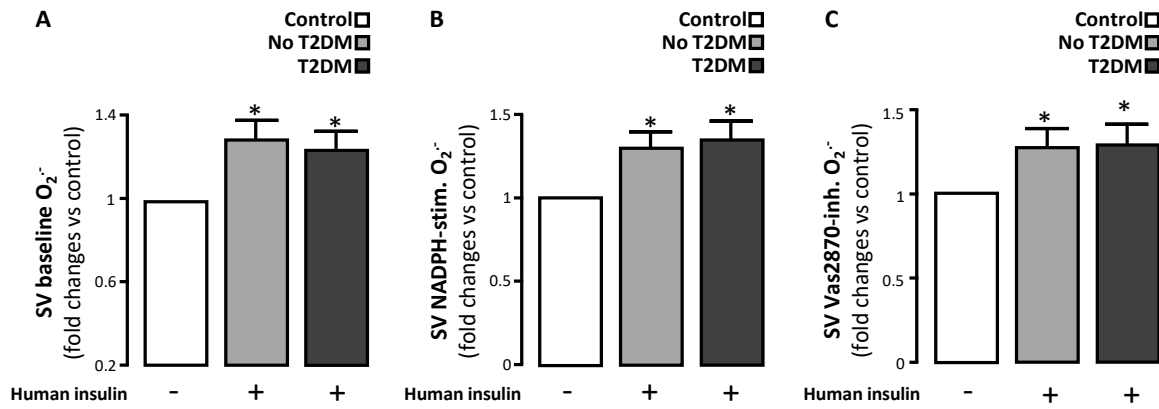
**Fig. S1. Direct effects of human insulin and insulin analogues on endothelial function ex vivo in humans.** (A-B) Effect of ex vivo insulin incubations [glargine M1 (10 nM), degludec (100 nM) or human insulin (10 nM)] on endothelium-dependent acetylcholine (ACh)-mediated vasorelaxations in saphenous vein (SV) segments from non-diabetic (A,  $n = 6$ ) and diabetic patients (B,  $n = 6$ ). (C-D) Effect of ex vivo insulin incubations [glargine M1 (10 nM), degludec (100 nM) or human insulin (10 nM)] on endothelium-independent sodium nitroprusside (SNP)-mediated vasorelaxations in SV from non-diabetic (C,  $n = 6$ ) and diabetic patients (D,  $n = 6$ ). HOMA-IR < 2.9 for all non-diabetic patients. \* $P < 0.05$  vs control, two-way ANOVA for matched observations for all panels. Data are presented as mean  $\pm$  SEM.



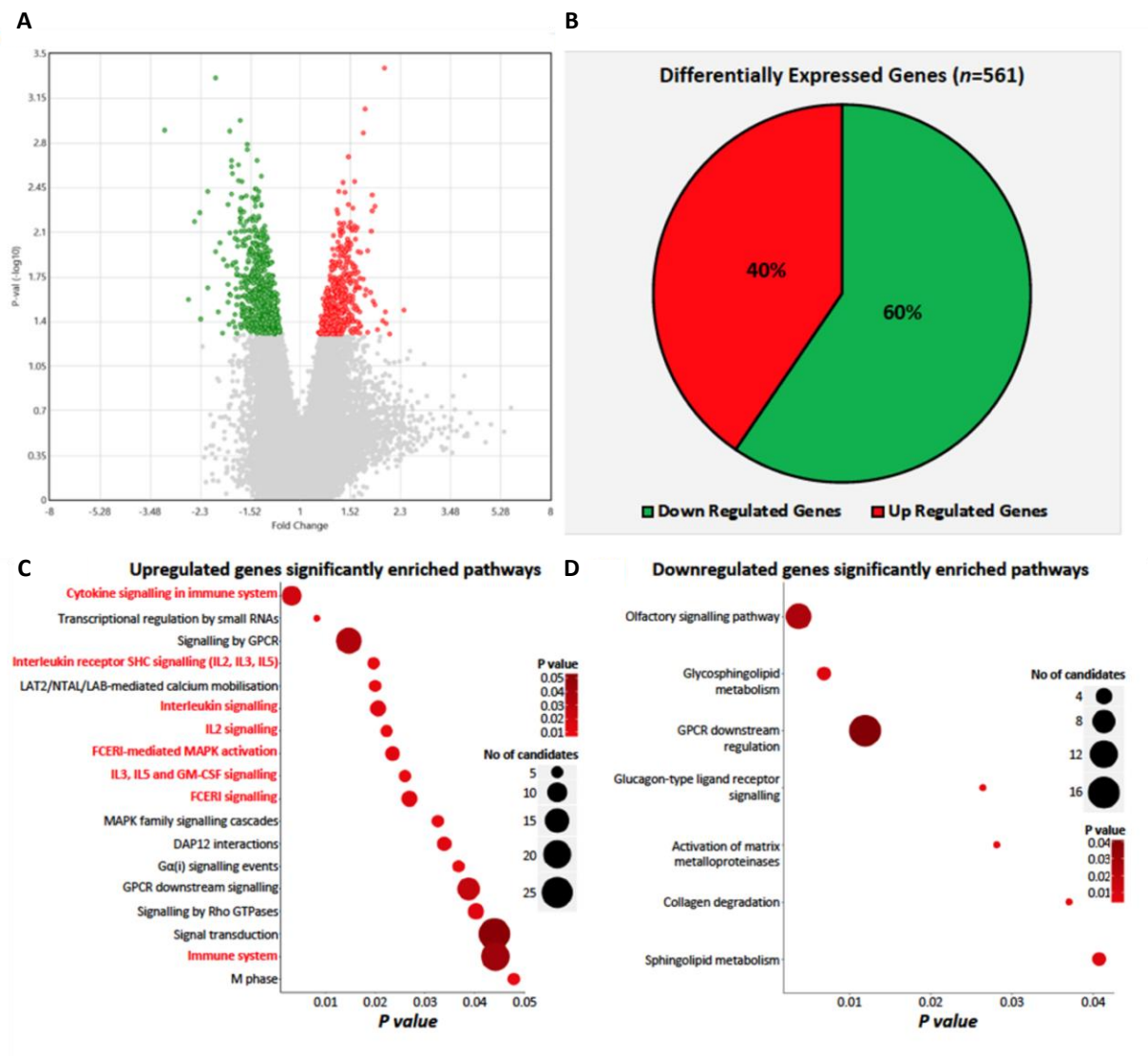
**Fig. S2. Association between serum insulin and NADPH-oxidases activity in humans. (A-B)** Association of serum insulin with NADPH-stimulated (A) and Vas2870-inhibitable (B) superoxide ( $O_2^{\cdot-}$ ) in saphenous vein (SV) segments from a subgroup of 173 patients from Study 1 without diabetes or evidence of systemic insulin resistance (IR, defined by HOMA-IR<2.9). **(C-D)** Association of serum insulin with NADPH-stimulated (C) and Vas2870-inhibitable (D) superoxide ( $O_2^{\cdot-}$ ) in internal mammary artery (IMA) segments in the aforementioned subgroup. *P*-values are calculated by Kruskal Wallis tests in all panels. Data are presented as median[25<sup>th</sup>-75<sup>th</sup> percentile].



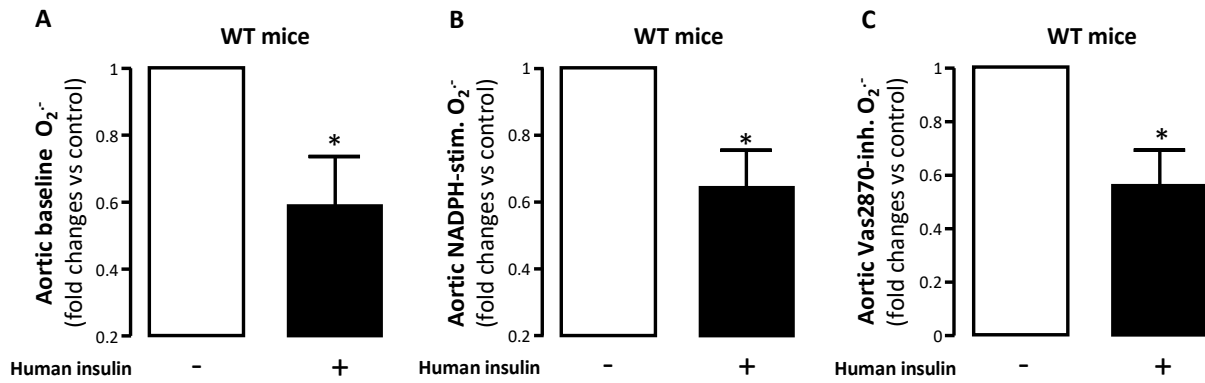
**Fig. S3. Dose-response effects of human insulin and insulin analogues on human vascular redox state.** (A-C) Dose-response effect of human insulin (1 nM, 10 nM, 100 nM) on basal (A), NADPH-stimulated (B) and Vas2870-inhibitable (C) superoxide ( $O_2^{\bullet-}$ ) in human saphenous vein (SV) segments. (D-F) Dose-response effect of insulin glargine (1 nM, 10 nM, 100 nM) on basal (D), NADPH-stimulated (E) and Vas2870-inhibitable (F)  $O_2^{\bullet-}$  in human SV. (G-I) Dose-response effect of insulin degludec (1 nM, 10 nM, 100 nM) on basal (G), NADPH-stimulated (H) and Vas2870-inhibitable (I)  $O_2^{\bullet-}$  in human SV). \* $P < 0.05$  vs control; \*\* $P < 0.017$  vs control by Wilcoxon sign rank tests ( $n = 10 - 20$  per intervention); data presented as mean  $\pm$  SEM.



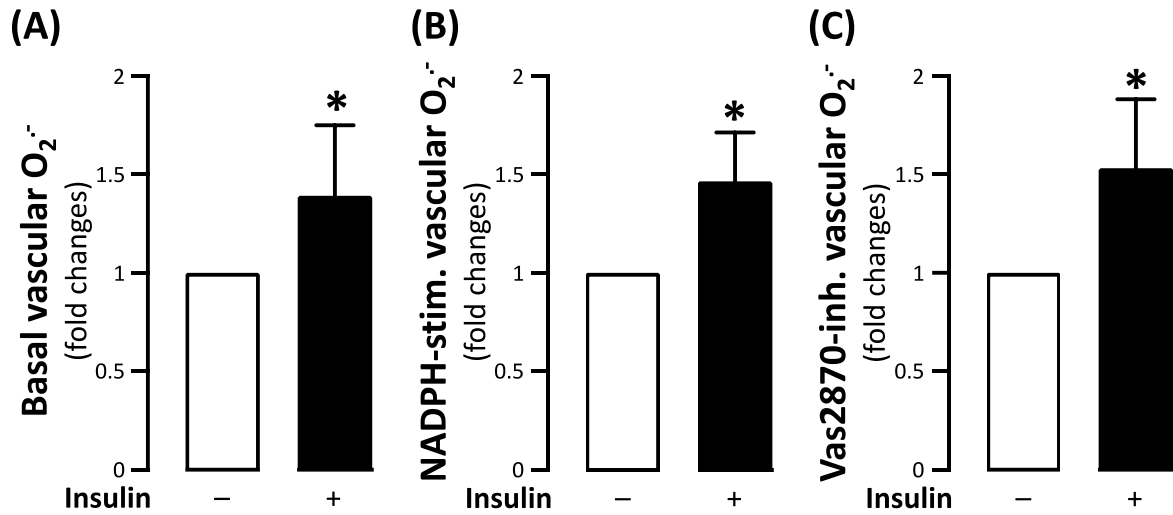
**Fig. S4. Effects of human insulin on vascular redox state in humans.** (A-C) Effect of human insulin (10nM) on basal (A,  $n = 7-12$  pairs), NADPH-stimulated (B,  $n = 7-12$  pairs) and Vas2870-inhibitable (C,  $n = 7-12$  pairs) superoxide ( $O_2^{\cdot-}$ ) in saphenous vein (SV) segments of patients with and without diabetes. \* $P < 0.05$  vs control. P-values are calculated by Wilcoxon sign rank tests in all panels (Bonferroni-adjusted). Data are presented as mean  $\pm$  SEM.



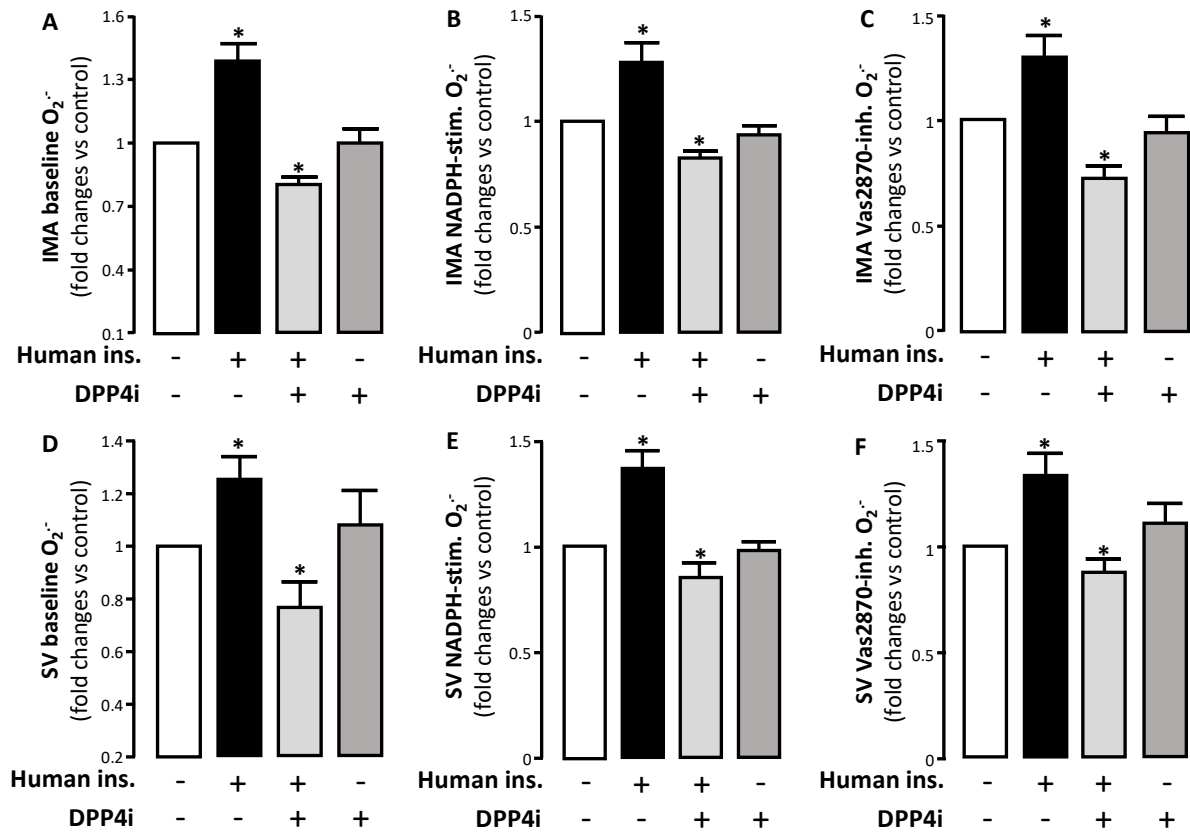
**Fig. S5. Effects of insulin on proinflammatory transcriptional pathways in human arteries.** (A) Volcano plot of the differentially expressed 561 genes in response to insulin (glargine, 10 nM for 8h,  $n = 6$ ). (B) Percentage of downregulated versus upregulated genes in response to insulin treatment.



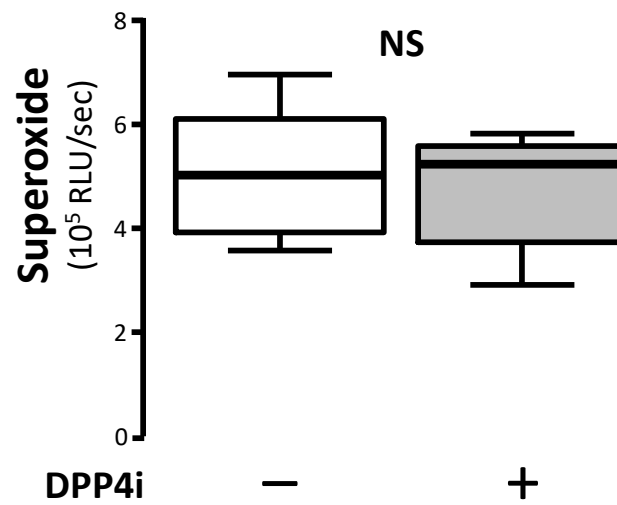
**Fig. S6. Effects of human insulin on vascular redox state in wild-type mice.** (A-C) Effect of human insulin (10 nM) on basal (A,  $n = 5$  pairs), NADPH-stimulated (B,  $n = 5$  pairs) and Vas2870-inhibitable (C,  $n = 5$ )  $O_2^-$  in aortic rings of atherosclerosis-free wild-type mice. \* $P < 0.05$  vs control. P-values are calculated by Wilcoxon sign rank tests in all panels (Bonferroni-adjusted). Data are presented as mean  $\pm$  SEM.



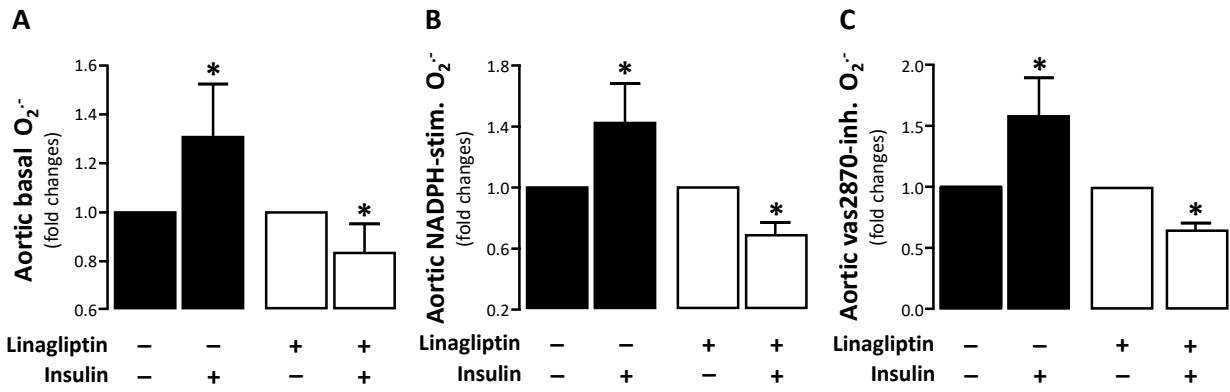
**Fig. S7. Effects of insulin on vascular redox state in diabetic patients on metformin.** (A-C) Effect of insulin (10 nM) on basal (A,  $n = 5$  pairs), NADPH-stimulated (B,  $n = 5$  pairs) and Vas2870-inhibitable (C,  $n = 5$  pairs) superoxide ( $O_2^{\bullet-}$ ) in diabetic patients on metformin treatment. \* $P < 0.05$  vs control.  $P$ -values are calculated by Wilcoxon sign rank tests; data presented as mean  $\pm$  SEM.



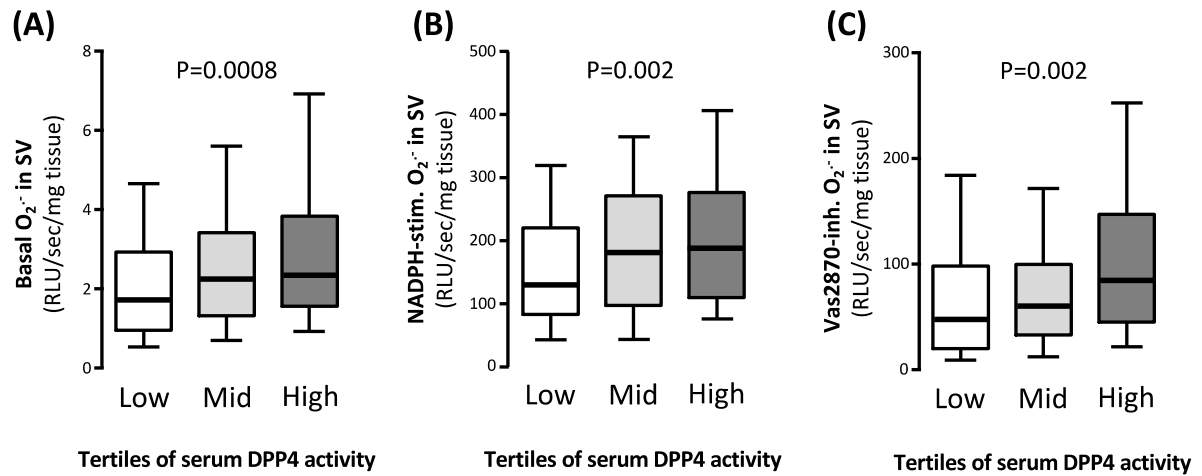
**Fig. S8. Dipeptidyl peptidase 4 inhibition (DPP4i) regulates the effects of human insulin on human vascular redox state.** (A-C) Effects of ex vivo human insulin (10 nM)/DPP4i treatments on basal (A,  $n = 8$ ), NADPH-stimulated (B,  $n = 8$ ) and Vas2870-inhibitable (C,  $n = 8$ )  $O_2^{\cdot-}$  in internal mammary artery (IMA) segments. (D-F) Effects of ex vivo human insulin (10 nM)/DPP4i treatments on basal (D), NADPH-stimulated (E) and Vas2870-inhibitable (F)  $O_2^{\cdot-}$  in SV ( $n = 8-18$  for D, E and F). \* $P < 0.05$  vs control.  $P$ -values are calculated by Wilcoxon sign rank tests in all panels (Bonferroni-adjusted). Data are presented as mean  $\pm$  SEM.



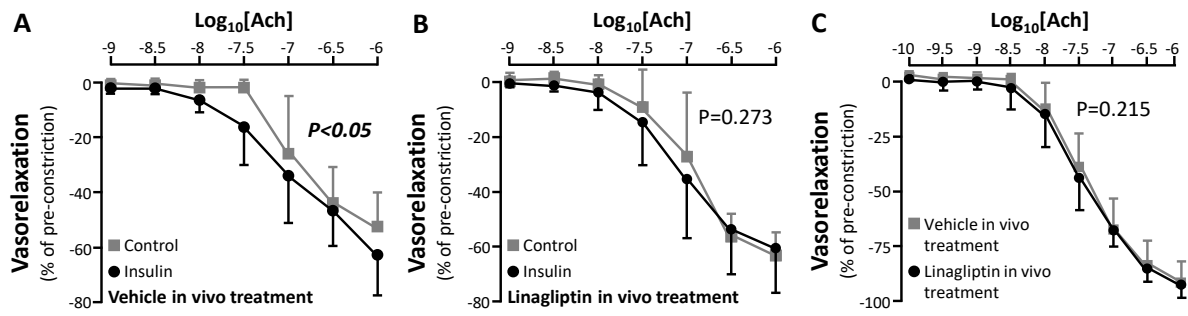
**Fig. S9. Dipeptidyl peptidase 4 inhibition has no direct superoxide ( $O_2^{\cdot-}$ )-scavenging properties.** Scavenging effect of DPP4i on  $O_2^{\cdot-}$  produced by the xanthine/xanthine oxidase system by lucigenin chemiluminescence. P-value calculated by Mann Whitney U test ( $n = 5$ ).



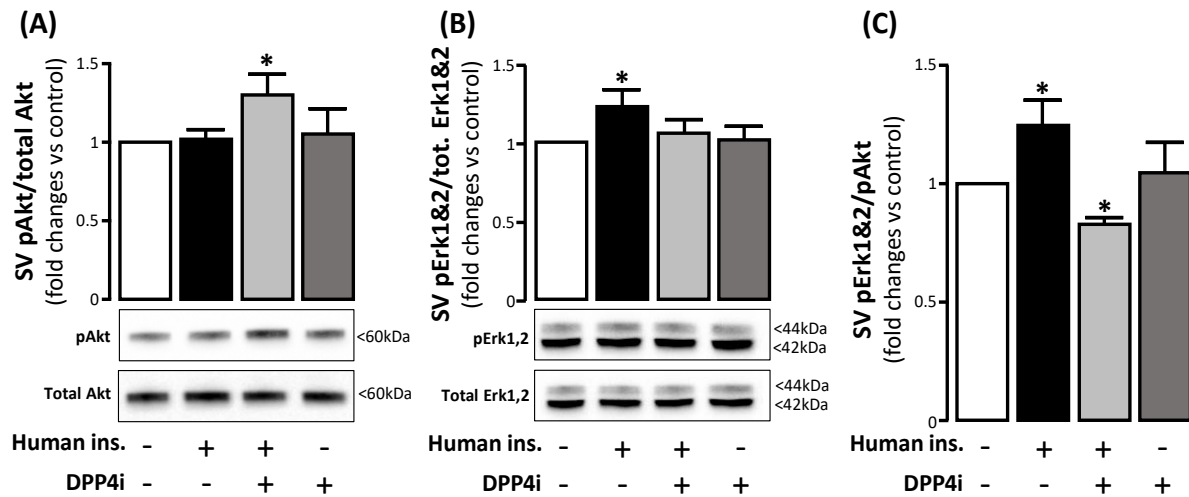
**Fig. S10. Linagliptin, a dipeptidyl peptidase 4 inhibitor, reverses the pro-oxidant effects of insulin on the vasculature of high fat diet (HFD)-fed ApoE<sup>-/-</sup> mice. (A-C)** Effect of in vivo linagliptin treatment on aortic basal (A, n = 5 per mouse group), NADPH-stimulated (B, n = 5 per mouse group) and Vas2870-inhibitable (C, n = 5 per mouse group)  $O_2^-$  in high fat diet (HFD)-fed ApoE<sup>-/-</sup> mice in response to ex vivo insulin (10 nM) treatment. \* $P < 0.05$  vs control by Wilcoxon sign rank tests in panels A-C; data presented as mean  $\pm$  SEM.



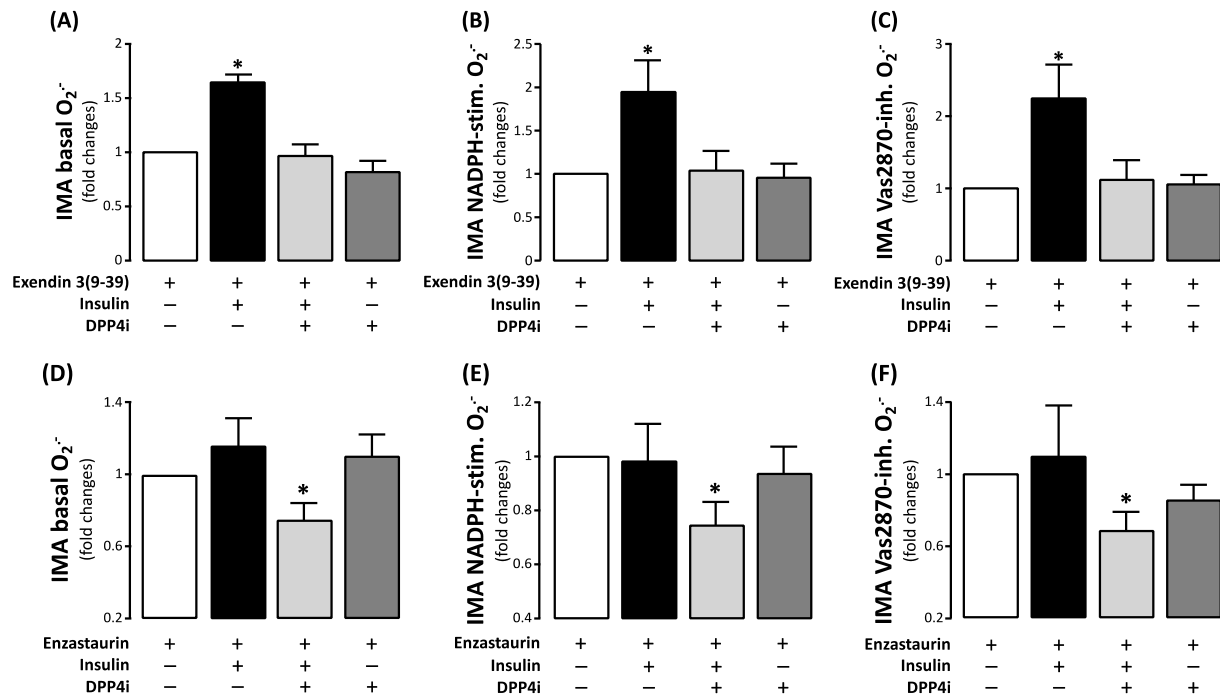
**Fig. S11. Association between circulating DPP4 activity and vascular redox state in humans. (A-C)** Association of circulating DPP4 activity with basal (A), NADPH-stimulated (B) and Vas2870-inhibitable (C) superoxide  $O_2^{\cdot-}$  in saphenous vein (SV) segments from Study 1 patients. Data are presented as 10<sup>th</sup>-90<sup>th</sup> percentile.  $P$ -values are calculated by Kruskal Wallis tests in all panels.



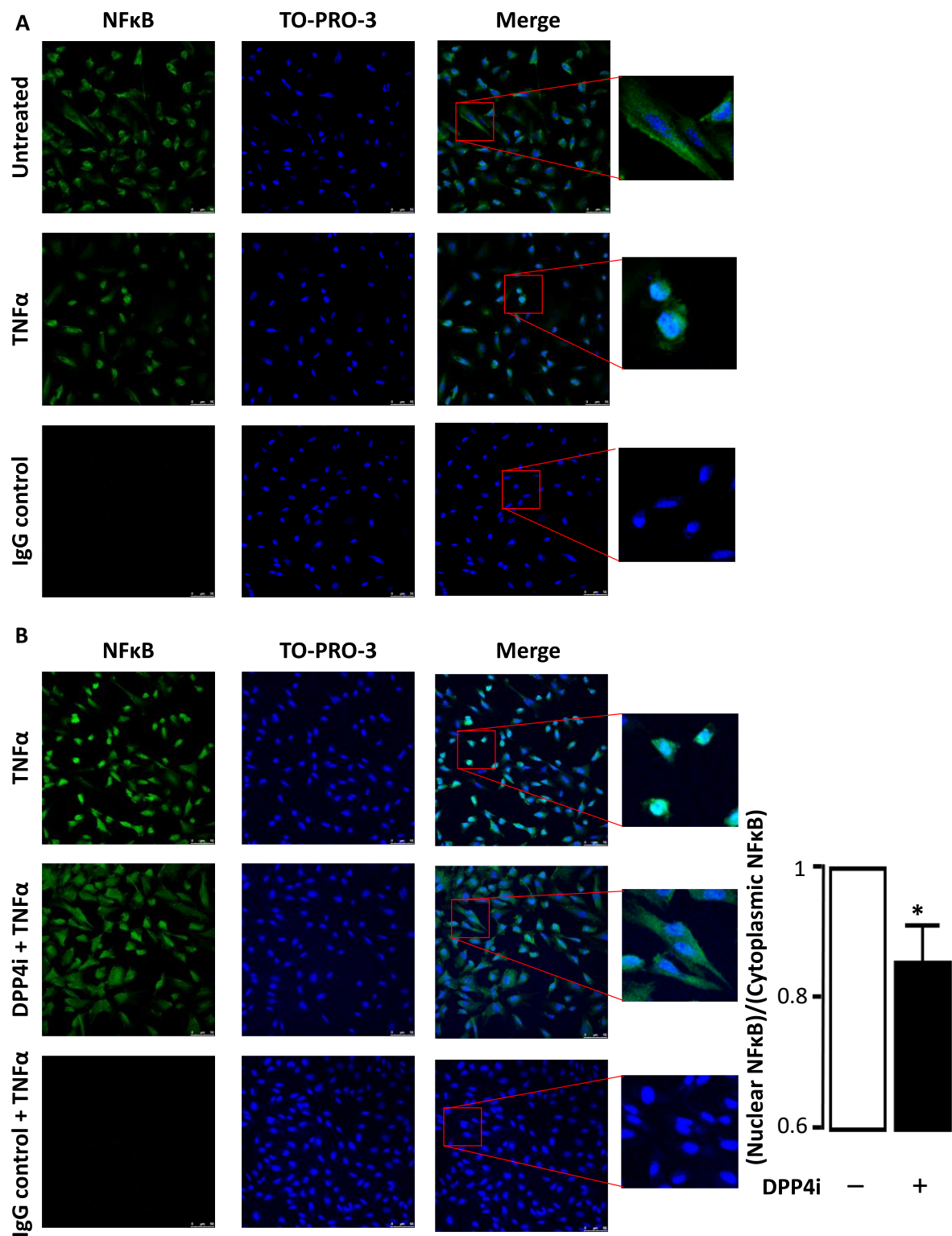
**Fig. S12. Linagliptin reverses the effect of insulin on endothelial function in high fat diet (HFD)-fed ApoE<sup>-/-</sup> mice. (A-B)** Effect of in vivo linagliptin treatment on endothelium-dependent acetylcholine vasorelaxations in response to insulin (10 nM) ex vivo in vehicle-treated (A, n = 5 per mouse group) versus linagliptin-treated (B, n = 5 per mouse group) HFD-fed ApoE<sup>-/-</sup> mice. **(C)** Endothelium-independent sodium nitroprusside (SNP) vasorelaxations in vehicle-treated versus linagliptin-treated (n = 5 per mouse group) HFD-fed ApoE<sup>-/-</sup> mice. *P*-values calculated by two-way ANOVA for repeated measures; data presented as mean ± SEM.



**Fig. S13. Dipeptidyl peptidase 4 inhibition (DPP4i) regulates the downstream signaling balance in response to human insulin in humans.** (A-C) Effect of ex vivo human insulin (10 nM)/DPP4i treatments on the downstream phosphorylation of Akt (A,  $n = 5$ ), Erk1&2 (B,  $n = 5$ ) and the balance of the two (C,  $n = 5$ ) in saphenous vein (SV) segments. \* $P < 0.05$  vs control by Wilcoxon sign rank tests; data presented as mean  $\pm$  SEM.

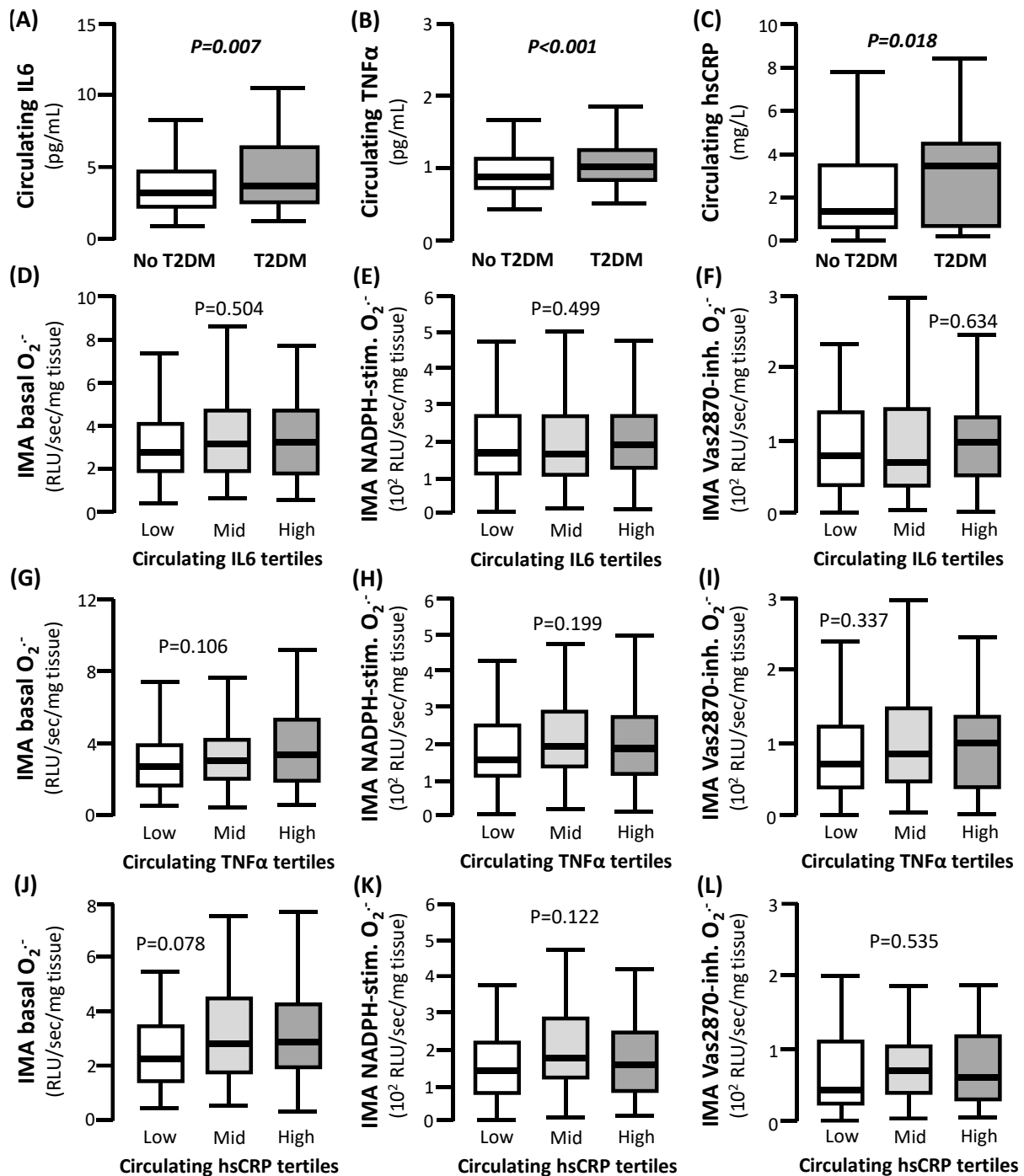


**Fig. S14. The role of glucagon like peptide 1 receptor (GLP1R) and protein kinase C $\beta$  (PKC $\beta$ ) signalling in the vascular insulin-sensitizing properties of dipeptidyl peptidase 4 inhibition (DPP4i). (A-C)** Effect of insulin (10 nM)/DPP4i ex vivo incubations on basal (A, n = 5), NADPH-stimulated (B, n = 5) and Vas2870-inhibitable (C, n = 5) superoxide ( $O_2^{\cdot-}$ ) in internal mammary artery (IMA) segments pre-treated with a GLP1R antagonist (exendin 3 (9-39 amide)). **(D-F)** Effect of insulin (10 nM)/DPP4i on basal (D, n = 5-7), NADPH-stimulated (E, n = 5-7) and Vas2870-inhibitable (F, n = 5-7)  $O_2^{\cdot-}$  in IMA segments pre-treated with a PKC $\beta$  inhibitor (enzastaurin). \* $P < 0.05$  vs control by Wilcoxon sign rank tests; data presented as mean  $\pm$  SEM.



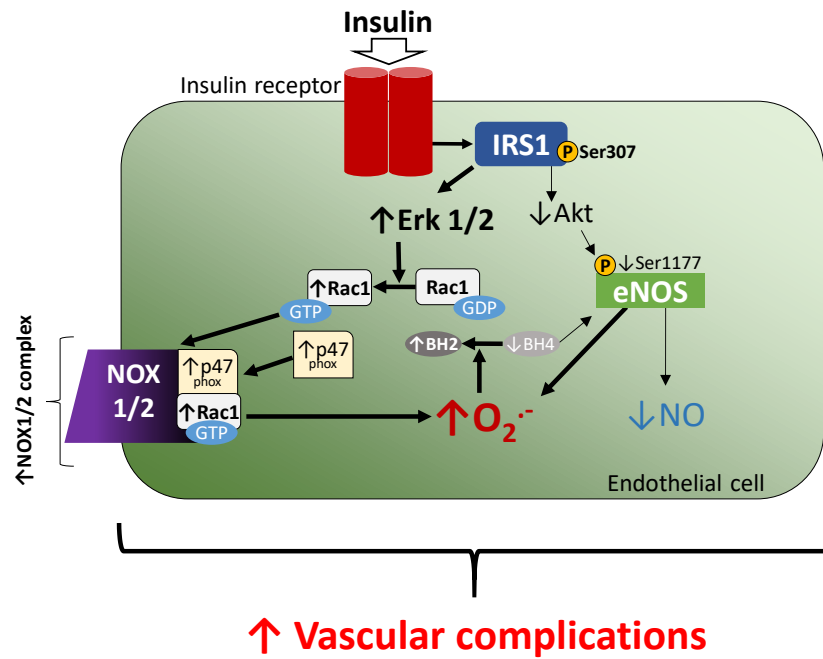
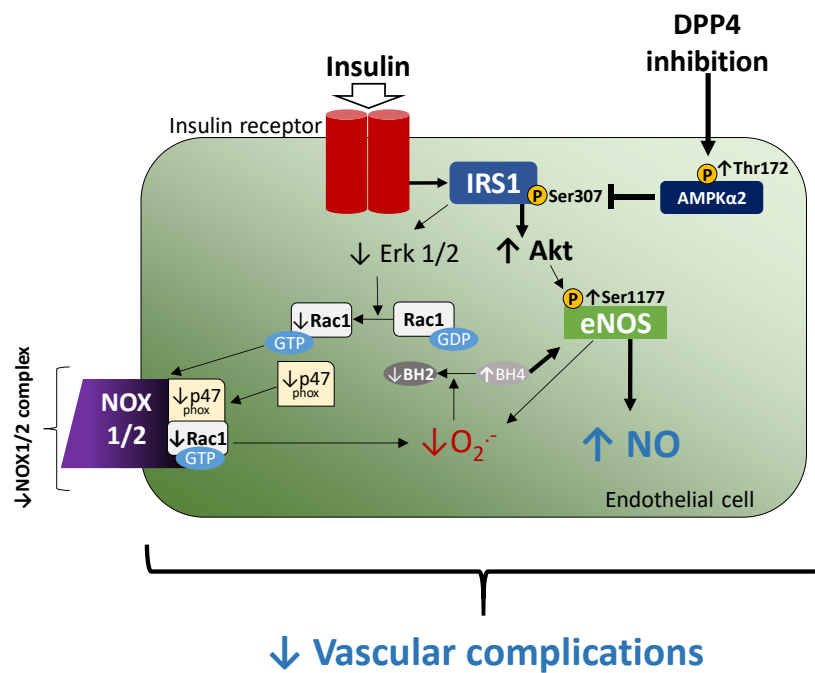
**Fig. S15. Effect of dipeptidyl peptidase 4 inhibition on nuclear factor kappa beta (NFκB) nuclear translocation.** (A) Confirmation of TNF-alpha-induced NF-kB activation and translocation to nucleus in HUVECs by immunofluorescence. Cells were grown either in absence (Untreated) or in the presence

of TNF-alpha (TNF- $\alpha$ ) and stained for NF- $\kappa$ B RelA (green) and nuclei (blue, TO-PRO-3). The specificity of NF- $\kappa$ B primary antibody staining was confirmed by incubating the cells with the corresponding isotype control (IgG control). Scale bar: 50  $\mu$ m. **(B)** Representative images of immunofluorescence with anti-NF- $\kappa$ B RelA antibody (green) on HUVECs treated with DPP4 inhibitor or without it (Untreated) and stimulated with TNF-alpha. Nuclei were stained with TO-PRO-3 (blue). Scale bar: 50  $\mu$ m. The bar chart shows the nuclear:cytoplasmic ratio of NF- $\kappa$ B RelA. Values are mean  $\pm$  SEM (n = 5). \* $P$  < 0.05, Wilcoxon sign rank test.



**Fig. S16. Proinflammatory cytokines, diabetes and arterial redox state in humans with atherosclerosis.** (A-C) Association of circulating interleukin 6 (IL6, A), tumour necrosis factor alpha (TNFα, B) and high sensitivity C-reactive protein (hsCRP, C) with diabetes in study 1. (D-F) Association of circulating IL6 with basal (D), NADPH-stimulated (E) and Vas2870-inhibitable (F) superoxide ( $O_2^{\cdot-}$ ) in study 1. (G-I) Association of circulating TNFα with basal (G), NADPH-stimulated (H) and Vas2870-inhibitable (I)  $O_2^{\cdot-}$  in study 1. (J-L) Association of circulating hsCRP with basal (J),

NADPH-stimulated (K) and Vas2870-inhibitable (L)  $O_2^-$  in study 1. *P*-values calculated by Mann Whitney U tests (A-C) or Kruskal Wallis tests (D-L); data presented as median[25th-75th percentile].

**A****B**

**fig. S17. Summary and proposed mechanism.** (A) Insulin presumably stimulates a disproportionate activation of Erk1&2 compared to the Akt signalling axis in the vascular wall

of humans with coronary atherosclerosis. This results in GTP-activation and membrane translocation of Rac1, which along with p47<sup>phox</sup> forms the active NADPH-oxidases complex, leading to increased oxidative stress, oxidation of tetrahydrobiopterin (BH<sub>4</sub>), uncoupling of endothelial nitric oxide synthase (eNOS), impairment of endothelial dysfunction and propagation of vascular complications. **(B)** DPP4 inhibition (DPP4i) increases vascular activation of AMP-activated kinase (AMPK), which restores insulin sensitivity by reducing the phosphorylation of insulin response substrate 1 (IRS1) at ser307 and reverses the vascular responses to insulin. The net effect includes marked insulin-mediated activation of Akt, activation (via phosphorylation) of eNOS combined with reduced oxidative stress and improved BH<sub>4</sub> availability. Vascular insulin sensitisation with a DPP4 inhibitor may be able to improve the *in vivo* cardiovascular effects of insulin treatment in diabetic patients, thus reducing the risk for long-term adverse cardiovascular events.

## Supplemental tables

**Table S1. Demographic characteristics of diabetic vs non-diabetic patients.** T2DM: Type 2 diabetes mellitus; BMI: Body mass index; hsCRP: High sensitivity C-reactive protein; ACEi: Angiotensin converting enzyme inhibitor; ARB: Angiotensin receptor blocker; Age and BMI are presented as mean  $\pm$  standard error; hsCRP is presented as median[25<sup>th</sup>-75<sup>th</sup> percentile]; Between-subgroup comparisons were made for each study by independent samples t-test or Mann Whitney U tests for continuous variables (depending on normality) and by Chi square tests for categorical variables; \* $P < 0.05$ , \*\* $P < 0.01$ , \*\*\* $P < 0.001$ .

|                              | Study 1         |                    | Study 2         |                   |
|------------------------------|-----------------|--------------------|-----------------|-------------------|
|                              | No T2DM         | T2DM               | No T2DM         | T2DM              |
| Participants (n)             | 443             | 123                | 60              | 28                |
| Age (years)                  | 67.4 $\pm$ 0.9  | 65.5 $\pm$ 1.0***  | 68.9 $\pm$ 1.3  | 67.1 $\pm$ 1.5    |
| Males (%)                    | 81.0            | 81.3               | 88.3            | 89.3              |
| Hypertension (%)             | 68.6            | 84.6***            | 78.0            | 78.6              |
| Hyperlipidaemia (%)          | 75.2            | 87.0**             | 90.0            | 100.0             |
| Smoking status               |                 |                    |                 |                   |
| - Active (%)                 | 9.0             | 13.8               | 10.0            | 0.0               |
| - Past (%)                   | 53.6            | 55.3               | 46.7            | 55.6              |
| BMI (kg/m <sup>2</sup> )     | 28.0 $\pm$ 0.2  | 30 $\pm$ 0.5***    | 27.7 $\pm$ 0.5  | 30.4 $\pm$ 0.5*** |
| Waist-to-hip ratio           | 0.97 $\pm$ 0.01 | 1.01 $\pm$ 0.01*** | 0.98 $\pm$ 0.01 | 1.00 $\pm$ 0.02   |
| Plasma hsCRP (mg/L)          | 1.3[0.6-3.5]    | 2.1[0.7-5.0]*      | 1.1[0.5-2.9]    | 1.2[0.5-2.0]      |
| <b>Medication</b>            |                 |                    |                 |                   |
| Antiplatelet (%)             | 79.9            | 87.8               | 86.2            | 77.8              |
| ACEi/ARB (%)                 | 59.8            | 69.1               | 67.2            | 70.4              |
| Statins (%)                  | 78.8            | 93.5***            | 87.7            | 88.5              |
| $\beta$ -blockers (%)        | 64.3            | 71.5               | 68.5            | 88.0              |
| Calcium channel blockers (%) | 22.3            | 37.4***            | 24.6            | 46.2              |
| Insulin (%)                  | 0.0             | 33.3***            | 0.0             | 26.9***           |
| Oral hypoglycaemic (%)       | 0.0             | 71.5***            | 0.0             | 80.8***           |

**Table S2. Multivariate regression analysis testing the interaction between insulin/DPP4 activity, use of statins, and plasma inflammatory biomarkers in predicting Vas2870-inhibitable superoxide ( $O_2^{\cdot-}$ ) in human internal mammary arteries (IMA)**

| Variable  | Bstand.             | Adjusted P value    |
|---|---------------------|---------------------|
| <b><i>High insulin &amp; high DPP4 activity</i></b> | <b><i>0.165</i></b> | <b><i>0.042</i></b> |
| Statin use  | −0.088              | 0.276               |
| Serum IL6   | 0.012               | 0.894               |
| Serum TNF $\alpha$                                  | 0.058               | 0.496               |
| Serum hsCRP   | 0.045               | 0.591               |

DPP4: Dipeptidyl peptidase 4; IL6: Interleukin 6; TNF $\alpha$ : Tumour necrosis factor alpha; hsCRP: High sensitivity C-reactive protein